Discover Oncology

Analysis

Identification of CWH43 as a novel prognostic biomarker and therapeutic target in clear cell renal cell carcinoma by a multi-omics approach and correlation with autophagy progression

Ailian Wu[1] · Peng Bai[2] · Hui Qu[3] · Tao Zhang[4]

Received: 17 January 2025 / Accepted: 14 April 2025
Published online: 15 June 2025

Abstract

Background Clear cell renal cell carcinoma (ccRCC) poses significant challenges due to its asymptomatic nature and poor prognosis at advanced stages. Identifying novel biomarkers is essential for enhancing prognostic accuracy and therapeutic strategies. This study explores the CWH43 gene, utilizing multi-omics data to determine its role in ccRCC.

Methods Genomic, transcriptomic, and methylation data from TCGA-KIRC and GEO databases were analyzed to evaluate CWH43 expression and clinical impact. Bioinformatics tools assessed correlations with patient outcomes and pathway involvement.

Results CWH43 expression was significantly reduced in ccRCC tissues and correlated with advanced disease stages and poor patient survival. Enrichment analyses revealed CWH43's involvement in critical cancer pathways, such as autophagy and immune response modulation, suggesting its significant role in ccRCC pathophysiology. Lower CWH43 levels were associated with increased tumor progression and immune evasion, impacting the tumor microenvironment.

Conclusion This study highlights the utility of multi-omics data in identifying CWH43 as a novel prognostic biomarker for ccRCC. Integrating CWH43 into clinical practice could refine prognostic assessments and guide personalized therapy strategies, aligning with advancements in modern oncology. Further research is warranted to explore CWH43's mechanisms and therapeutic potential.

Keywords CWH43 · CcRCC · Immunotherapy response biomarkers · Tumor-immune interactions · Tumor microenvironment · Next-generation sequencing technologies · Cancer immunology · Therapeutic targets in immunotherapy

Ailian Wu and Peng Bai have contributed equally to this work. Hui Qu and Tao Zhang are the corresponding authors of the article.

Supplementary Information The online version contains supplementary material available at https://doi.org/10.1007/s12672-025-02392-8.

✉ Hui Qu, 13518292979@163.com; ✉ Tao Zhang, chris2111 @163.com | [1]School of Medicine, Yangzhou Polytechnic College, Yangzhou, China. [2]Department of Ultrasonography, Ya'an People's Hospital, Yaan 625000, China. [3]Department of Radiology, Xichong People's Hospital, Nanchong 637200, China. [4]Department of Urology, Shandong Provincial Hospital Affliated to ShandongFirst Medical University, Jinan 250021, China.

1 Introduction

Renal cell carcinoma (RCC) ranks as the third most prevalent cancer within the genitourinary tract, trailing only prostate and bladder cancers, and has displayed a rising trend over the last decade [1]. Among the RCC subtypes, clear cell RCC (ccRCC) predominates, comprising 85% of cases and is the principal cause of mortality in this patient group [2]. In its initial stages, ccRCC typically remains asymptomatic, with 20 to 30% of cases being advanced or metastatic at diagnosis [3]. Treatment challenges intensify for patients with advanced, recurrent, or metastatic ccRCC; these patients often exhibit a poor response to radiotherapy and chemotherapy, endure high recurrence rates, and face a bleak prognosis [4]. Consequently, the prognosis for diagnosing and managing clear cell renal cell carcinoma (ccRCC) remains rather challenging. However, recent comprehensive studies into the origins and progression of ccRCC have shed new light on its pathogenesis. These investigations have identified numerous epigenetic modifications, particularly aberrant DNA methylation, as playing a pivotal role in disease development and significantly correlating with patient outcomes. [5]. Tumor immunotherapy, which seeks to harness and amplify the body's immune defenses to eradicate cancer cells, has emerged as a pivotal advance in enhancing the survival rates of ccRCC patients in recent years [6]. Key to this approach are certain immune checkpoints that, by curbing immune cell activity, facilitate tumor cells to evade immune detection, thus thwarting an effective immune response [7]. Identifying novel prognostic indicators and therapeutic targets for ccRCC thus remains essential for improving patient survival outcomes in renal cell carcinoma.

CWH43, known as the CWH43-C or PGAP2-interacting protein, resides on chromosome 4 and belongs to the human CCDS set. This protein plays a role in the biosynthesis of glycosylphosphatidylinositol (GPI)-anchored molecules [8]. Evidence suggests a reduction in CWH43 expression in tissues from colorectal tumors [9; 10]. Additionally, its association with the development of thyrotropin-secreting pituitary adenomas has been observed, though the underlying mechanisms remain undefined [11]. Ye and colleagues have identified the presence of cancer-specific super-enhancers involving CWH43 in esophageal squamous cell carcinoma [12]. These findings indicate that CWH43 could serve as a promising predictive and prognostic biomarker in oncology, potentially enhancing treatment strategies and forecasting patient survival rates. Nonetheless, the specific roles and mechanisms of CWH43 in tumor progression and its impact on tumor immunology have yet to be fully elucidated, particularly its relevance to clear cell renal cell carcinoma (ccRCC) remains unexplored.

In this study, we initially assessed the expression levels, clinicopathological features, and prognostic significance of CWH43 in patients with clear cell renal cell carcinoma (ccRCC) using data from The Cancer Genome Atlas (TCGA) and other relevant databases. We further constructed a nomogram incorporating calibration curves to predict the survival probabilities at 1, 3, and 5 years for patients with ccRCC. Our analysis also explored the associations between CWH43 expression, methylation patterns, and gene mutations, as well as their prognostic implications in ccRCC. Moreover, we evaluated the sensitivity of CWH43 to various drugs using the CellMiner software.

Crucially, this study marks the first extensive multidimensional analysis of CWH43's immunological implications, revealing its role in promoting an inflammatory tumor microenvironment (TME) in ccRCC. To delve deeper into the biological functions of CWH43 in ccRCC pathogenesis, we conducted analyses using Gene Ontology (GO) terms and the Kyoto Encyclopedia of Genes and Genomes (KEGG) pathways. Given that the enrichment analyses highlighted a connection with autophagy, we further investigated the relationship between CWH43 expression and autophagic processes.

In summary, our research comprehensively clarifies the role and mechanistic interactions of CWH43 in ccRCC and tumor immunity, proposing that CWH43 could serve as a novel prognostic biomarker and a potential target for immunotherapy in ccRCC.

2 Method

2.1 Patient data sets

RNA sequencing and clinical data for kidney clear cell carcinoma (KIRC) were retrieved from the TCGA database in HTSeq-FPKM format (https://portal.gdc.cancer.gov/), and subsequently, the RNAseq data were transformed from

FPKM (Fragments Per Kilobase of transcript per Million mapped reads) to TPM (transcripts per million reads) and log2 normalized. Data encompassing 611 KIRC projects, including 72 samples with matched adjacent tissues, were analyzed. Furthermore, RNAseq data in TPM format were obtained from UCSC XENA (https://xenabrowser.net/datapages/) [13], processed uniformly through the Toil framework to align with both TCGA and GTEx standards. This study involved extracting and comparing RNAseq data between KIRC and normal tissue samples from GTEx, focusing on TPM formatted and log2-transformed expression profiles.

Additional datasets, specifically GSE46699, GSE53757, GSE66270, and GSE66271, were sourced from the GEO database (https://www.ncbi.nlm.nih.gov/geo/) utilizing the R GEOquery package [14]. Differential expression analysis was conducted with the limma package, applying criteria of $|logFC| > 2$ and an adjusted P-value < 0.05 to determine significant differences between normal and tumor samples. This analysis particularly highlighted the expression patterns of CWH43 in KIRC, comparing tumor versus normal groups. Genes related to autophagy were sourced from the Human Autophagy Database (http://hamdb.scbdd.com) [15], enriching our understanding of their roles in KIRC pathophysiology.

2.2 Survival analysis

Patients with clear cell renal cell carcinoma (ccRCC) were stratified into two groups based on the median expression levels of the CWH43 gene: a high expression group and a low expression group. The association between CWH43 expression and patient outcomes, including overall survival (OS), disease-specific survival (DSS), and progression-free interval (PFI), was examined using Kaplan–Meier curves [16]. Furthermore, the relationship between CWH43 expression and disease-free survival (DFS) in ccRCC patients was assessed using the GEPIA database (http://gepia.cancer-pku.cn/) [17]. Hazard ratios (HRs) and 95% confidence intervals were determined through univariate survival analysis to quantify the impact of CWH43 expression levels on survival metrics.

2.3 Methylation and gene mutation analysis of CWH43 in ccRCC

The UALCAN database (http://ualcan.path.uab.edu/analysis-prot.html) [18], a comprehensive platform for the analysis of TCGA gene expression data, was employed to explore the relationship between CWH43 DNA methylation levels and clinicopathological characteristics in patients with clear cell renal cell carcinoma (ccRCC). We further leveraged the TCGA database in conjunction with the Illumina Human Methylation 450 platform (Illumina, San Diego, CA, USA) to investigate the association between CWH43 expression and DNA methylation patterns at specific genomic loci. Moreover, the prognostic significance of CWH43 methylation levels in ccRCC was assessed using the MethSurv database (https://biit.cs.ut.ee/methsurv/) [19].

Mutation data for CWH43 were sourced from the cBioPortal (http://cbioportal.org) [20]. We analyzed the genomic alterations of CWH43 applying a z-score threshold of ± 1.5 to evaluate the extent of gene expression changes due to mutations. Additionally, the impact of CWH43 mutations on the overall survival of ccRCC patients was examined to ascertain their potential prognostic value.

2.4 Correlation analysis of CWH43 expression and drug sensitivity

The analysis of the relationship between CWH43 expression and drug sensitivity was conducted using the CellMiner database (http://discover.nci.nih.gov/cellminer/) [21, 22]. To process this data and generate the relevant graphs, we employed several packages within the R programming environment. Specifically, the"impute"package was utilized for handling missing values, the"limma"package for conducting differential expression analysis, and the"ggpubr"package for creating publication-quality graphics. This methodology allowed for a detailed exploration of how variations in CWH43 expression influence the response to pharmacological treatments.

2.5 Tumor microenvironment analysis

To elucidate the tumor microenvironment in clear cell renal cell carcinoma (ccRCC) samples, we analyzed 122 immunomodulators such as MHC molecules, receptors, chemokines, and immune stimulants, drawing from the work of Charoentong et al. [23]. Visualization of these data was achieved through the creation of a heat map using the'pheatmap'package in R. Additionally, we accessed a cancer immune cycle-related gene set from Xu et al.'s online resource (http://biocc.hrbmu.edu.cn/TIP/) [24], and a gene signature indicative of a positive clinical response to the

anti-PD-L1 therapy atezolizumab, as identified in the research by Mariathasan [25]. The ssGSEA algorithm was employed to calculate enrichment scores for these gene signatures.

Our analysis extended to exploring the relationship between the expression of CWH43 and the dynamics of the cancer-immune cycle, including predictions of responses to immunotherapy. The ESTIMATE algorithm was used to evaluate the tumor microenvironment's composition for each sample [25], quantifying immune cell infiltration (immune score), stromal content (stromal score), a combined stromal-immune score (estimated value score), and tumor purity. Furthermore, the CIBERSORT algorithm [26] was applied to determine differences in immune cell proportions between patient groups with high and low expression of CWH43.

2.6 Enrichment analysis

Using the 'limma' R package [27], we identified genes that are differentially expressed between groups with high and low CWH43 expression. A co-expression heat map illustrating the relationships between CWH43 and the top 20 differentially expressed genes was constructed using Pearson correlation coefficients. Subsequent GO and KEGG enrichment analyses were performed with the 'clusterProfiler' R package [28], adhering to a significance threshold of a P-value < 0.05. The GO enrichment analysis elucidated the biological processes (BP), cellular components (CC), and molecular functions (MF) related to these genes, providing insights into their roles within cellular activities. Similarly, KEGG pathway analysis detailed the biological pathways implicated by these genes, offering a broader understanding of their functional integrations and potential impacts on cellular and systemic levels..

2.7 Statistical analysis

Statistical analyses were performed using the R software, version 4.2.2, 64-bit edition, equipped with essential support packages. To evaluate differences between two groups for continuous variables, the non-parametric Wilcoxon rank sum test was utilized. Additionally, Spearman correlation analysis was employed to determine correlation coefficients among variables. For all statistical tests conducted within this study, a P-value of less than 0.05 was established as the threshold for statistical significance.

3 3. Result

3.1 Variation in CWH43 expression between tumor and normal tissues

We examined CWH43 expression in 539 tumor specimens and 72 normal tissues, discovering a significantly reduced expression of CWH43 in tumor samples relative to normal counterparts as per TCGA data (p = 1.7e-37) (Fig. 1A). Furthermore, we assessed CWH43 expression differences between normal and ccRCC tissues adjacent to ccRCC using combined data from TCGA and GTEx, observing that CWH43 levels were substantially lower in ccRCC than in adjacent normal tissues (p = 9e-43) (Fig. 1B). Similarly, a comparison of 72 matched ccRCC and neighboring samples revealed a significant decrease in CWH43 expression in the tumor samples (p = 2.4e-12) (Fig. 1C).

To evaluate CWH43's diagnostic potential for ccRCC, we conducted receiver operating characteristic (ROC) analysis of CWH43 expression in ccRCC and adjacent normal samples, integrating GTEx data. The areas under the curve (AUC) consistently exceeded 0.9, suggesting CWH43's utility as a moderately effective biomarker for ccRCC (Fig. 1D-E).

Additionally, we explored quantitative differences in CWH43 protein expression using the Ualcan database, confirming lower levels of this protein in ccRCC tissues (p = 3.9e-03) (Fig. 1F). Further analysis through human protein profiles reinforced the observation of diminished CWH43 protein levels in ccRCC compared to normal tissues (Fig. 1G-H).

3.2 Link between CWH43 gene expression and clinicopathological traits in ccRCC patients

Table 1 details the clinicopathological features of 539 ccRCC patients, as recorded in the TCGA database. These patients were categorized based on the median expression of CWH43 into two groups: a high expression group (n = 270) and a low expression group (n = 269). The association between levels of CWH43 expression and clinicopathological traits was examined using chi-square test, Fisher's exact test, and Wilcoxon signed-rank sum test. Our findings indicate a significant correlation of CWH43 expression with several clinical parameters: age (p = 8.3e-03) (Fig. 2A), gender (p = 3e-03) (Fig. 2B), T

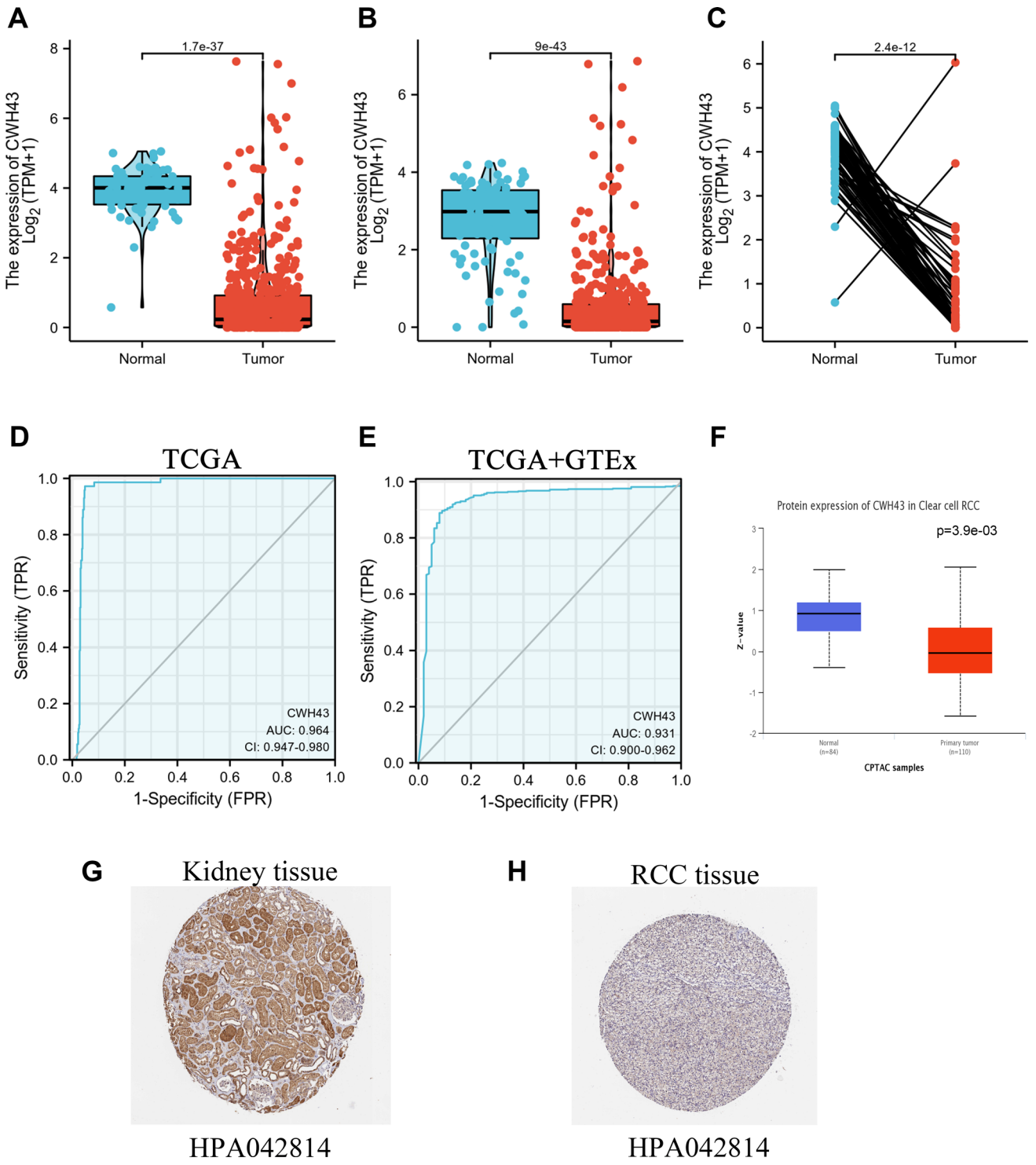

Fig. 1 Differential Expression of CWH43 in ccRCC and Normal Tissues. **A** A Wilcoxon rank sum test assessed the variation in CWH43 expression between ccRCC and adjacent normal tissues. **B** This statistical test also evaluated CWH43 levels across normal adjacent tissues from the GTEx and ccRCC tissues from the TCGA databases. **C** Comparison of CWH43 expression in 72 paired ccRCC and adjacent normal samples. **D**, **E** ROC curves illustrating the diagnostic ability of CWH43 expression to differentiate between ccRCC and non-tumor tissue; the false positive rate is plotted on the X-axis against the true positive rate on the Y-axis. **F** Ualcan database analysis of CWH43 protein levels in ccRCC versus normal tissues. **G**, **H** Comparative levels of CWH43 protein in ccRCC and normal tissues, as indicated in the Human Protein Atlas (Antibody HPA042814, magnification 10X)

Table 1 Correlation between CWH43 expression and clinicopathological characteristics in ccRCC

Characteristic	Low expression of CWH43	High expression of CWH43	p
n	269	270	
Age, n (%)			0.182
< = 60	126 (23.4%)	143 (26.5%)	
> 60	143 (26.5%)	127 (23.6%)	
Gender, n (%)			0.016
Female	79 (14.7%)	107 (19.9%)	
Male	190 (35.3%)	163 (30.2%)	
Race, n (%)			0.609
Asian	4 (0.8%)	4 (0.8%)	
Black or African American	25 (4.7%)	32 (6%)	
White	237 (44.5%)	230 (43.2%)	
T stage, n (%)			< 0.001
T1	111 (20.6%)	167 (31%)	
T2	42 (7.8%)	29 (5.4%)	
T3	107 (19.9%)	72 (13.4%)	
T4	9 (1.7%)	2 (0.4%)	
N stage, n (%)			0.149
N0	128 (49.8%)	113 (44%)	
N1	12 (4.7%)	4 (1.6%)	
M stage, n (%)			0.019
M0	204 (40.3%)	224 (44.3%)	
M1	49 (9.7%)	29 (5.7%)	
Pathologic stage, n (%)			< 0.001
Stage I	107 (20%)	165 (30.8%)	
Stage II	33 (6.2%)	26 (4.9%)	
Stage III	74 (13.8%)	49 (9.1%)	
Stage IV	52 (9.7%)	30 (5.6%)	
Primary therapy outcome, n (%)			0.038
PD	7 (4.8%)	4 (2.7%)	
SD	0 (0%)	6 (4.1%)	
PR	0 (0%)	2 (1.4%)	
CR	52 (35.4%)	76 (51.7%)	
Histologic grade, n (%)			< 0.001
G1	1 (0.2%)	13 (2.4%)	
G2	95 (17.9%)	140 (26.4%)	
G3	125 (23.5%)	82 (15.4%)	
G4	47 (8.9%)	28 (5.3%)	
Serum calcium, n (%)			0.271
Elevated	6 (1.6%)	4 (1.1%)	
Low	107 (29.2%)	96 (26.2%)	
Normal	69 (18.9%)	84 (23%)	
Hemoglobin, n (%)			0.120
Elevated	2 (0.4%)	3 (0.7%)	
Low	145 (31.6%)	118 (25.7%)	
Normal	87 (19%)	104 (22.7%)	
Laterality, n (%)			0.229
Left	133 (24.7%)	119 (22.1%)	
Right	135 (25.1%)	151 (28.1%)	
Age, meidan (IQR)	62 (52, 71)	60 (51.25, 69)	0.204

Table 1 (continued)

Characteristics	Total(N)	Odds Ratio(OR)	P value
Age (> 60 vs. < = 60)	539	0.783 (0.557–1.097)	0.155
Gender (Male vs. Female)	539	0.633 (0.442–0.905)	0.012
Race (White vs. Asian&Black or African American)	532	0.782 (0.461–1.315)	0.355
T stage (T3&T4 vs. T1&T2)	539	0.498 (0.346–0.712)	< 0.001
N stage (N1 vs. N0)	257	0.378 (0.103–1.118)	0.100
M stage (M1 vs. M0)	506	0.539 (0.325–0.880)	0.015
Pathologic stage (Stage III&Stage IV vs. Stage I&Stage II)	536	0.460 (0.321–0.655)	< 0.001
Primary therapy outcome (CR vs. PD&SD&PR)	147	0.853 (0.300–2.266)	0.754
Histologic grade (G3&G4 vs. G1&G2)	531	0.401 (0.282–0.568)	< 0.001
Serum calcium (Low vs. Elevated)	213	1.346 (0.373–5.397)	0.653
Hemoglobin (Low vs. Elevated)	268	0.543 (0.071–3.325)	0.507
Laterality (Right vs. Left)	538	1.250 (0.891–1.756)	0.197

stage (p = 4.8e-06) (Fig. 2C), M stage (p = 0.01) (Fig. 2D), pathological stage (p = 5.8e-07) (Fig. 2E), and histological grade (p = 6.6e-09) (Fig. 2F). However, no significant correlations were observed with other clinical features (Supplementary Fig. 1).

Additionally, logistic regression analysis was conducted to further delineate the relationships between CWH43 expression and the clinicopathological characteristics of ccRCC patients, presented in Table 2. The analysis confirmed significant

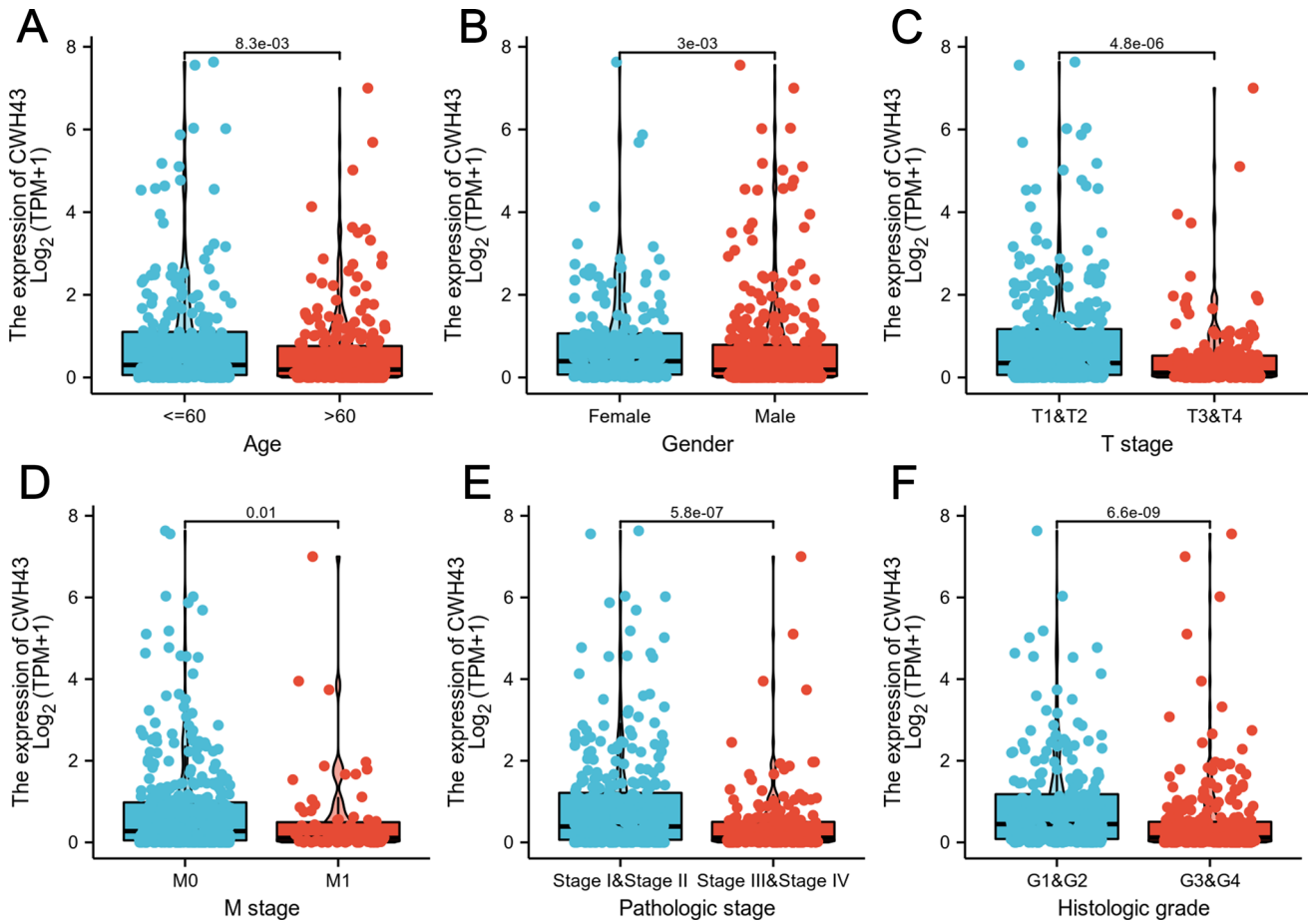

Fig. 2 Correlations Between CWH43 Expression and Clinical Variables in ccRCC. **A** Age, (**B**) Gender, (**C**) Tumor (**T**) stage, (**D**) Metastasis (**M**) stage, (**E**) Pathological stage, (**F**) Histological grade

Table 2 CWH43 Expression Associated with Clinicopathologic Characteristics (Logistic Regression)

Characteristics	Total(N)	Univariate analysis		Multivariate analysis	
		Hazard ratio (95% CI)	P value	Hazard ratio (95% CI)	P value
Age	539				
< = 60	269	Reference			
> 60	270	1.765 (1.298–2.398)	< 0.001	1.621 (1.053–2.495)	0.028
Gender	539				
Female	186	Reference			
Male	353	0.930 (0.682–1.268)	0.648		
Race	532				
Asian & Black or African American	65	Reference			
White	467	1.222 (0.678–2.201)	0.505		
T stage	539				
T1&T2	349	Reference			
T3&T4	190	3.228 (2.382–4.374)	< 0.001	1.924 (0.838–4.420)	0.123
N stage	257				
N0	241	Reference			
N1	16	3.453 (1.832–6.508)	< 0.001	1.635 (0.808–3.305)	0.171
M stage	506				
M0	428	Reference			
M1	78	4.389 (3.212–5.999)	< 0.001	2.849 (1.640–4.947)	< 0.001
Pathologic stage	536				
Stage I & Stage II	331	Reference			
Stage III & Stage IV	205	3.946 (2.872–5.423)	< 0.001	0.976 (0.378–2.520)	0.961
Histologic grade	531				
G1 & G2	249	Reference			
G3 & G4	282	2.702 (1.918–3.807)	< 0.001	1.469 (0.876–2.463)	0.145
Laterality	538				
Left	252	Reference			
Right	286	0.706 (0.523–0.952)	0.023	1.162 (0.747–1.809)	0.506
CWH43	539				
Low	269	Reference			
High	270	0.492 (0.361–0.671)	< 0.001	0.543 (0.335–0.881)	0.013

associations of CWH43 expression with gender (p = 0.012), T stage (p = < 0.001), M stage (p = 0.015), pathological stage (p < 0.001), and histological stage (p < 0.001). These results underscore the potential role of CWH43 as a biomarker linked to specific clinical outcomes in ccRCC.

3.3 Association of low CWH43 expression with adverse prognostic outcomes in ccRCC patients

Analysis of the TCGA-KIRC dataset revealed that low CWH43 expression correlates significantly with poor outcomes across multiple survival metrics. Specifically, patients with low expression exhibited markedly reduced overall survival (OS) (p < 0.001) (Fig. 3A), disease-specific survival (DSS) (p < 0.001) (Fig. 3B), and progression-free interval (PFI) (p < 0.001) (Fig. 3C). Further investigation using the GIPIA2 database also demonstrated a significant association between low CWH43 expression and reduced disease-free survival (DFS) (p = 0.00014) (Fig. 3D).

Utilizing a Cox univariate regression model, significant variables impacting prognosis included age > 60 years (p < 0.001), advanced T stages (T3 & T4) (p < 0.001), nodal involvement (N1) (p < 0.001), metastasis (M1) (p < 0.001), late-stage disease (Stage III & IV) (p < 0.001), high-grade tumors (G3 & G4) (p < 0.001), and tumor location (Right) (p = 0.023), along with high CWH43 expression (p < 0.001). To consolidate these findings, multivariate risk analysis was conducted

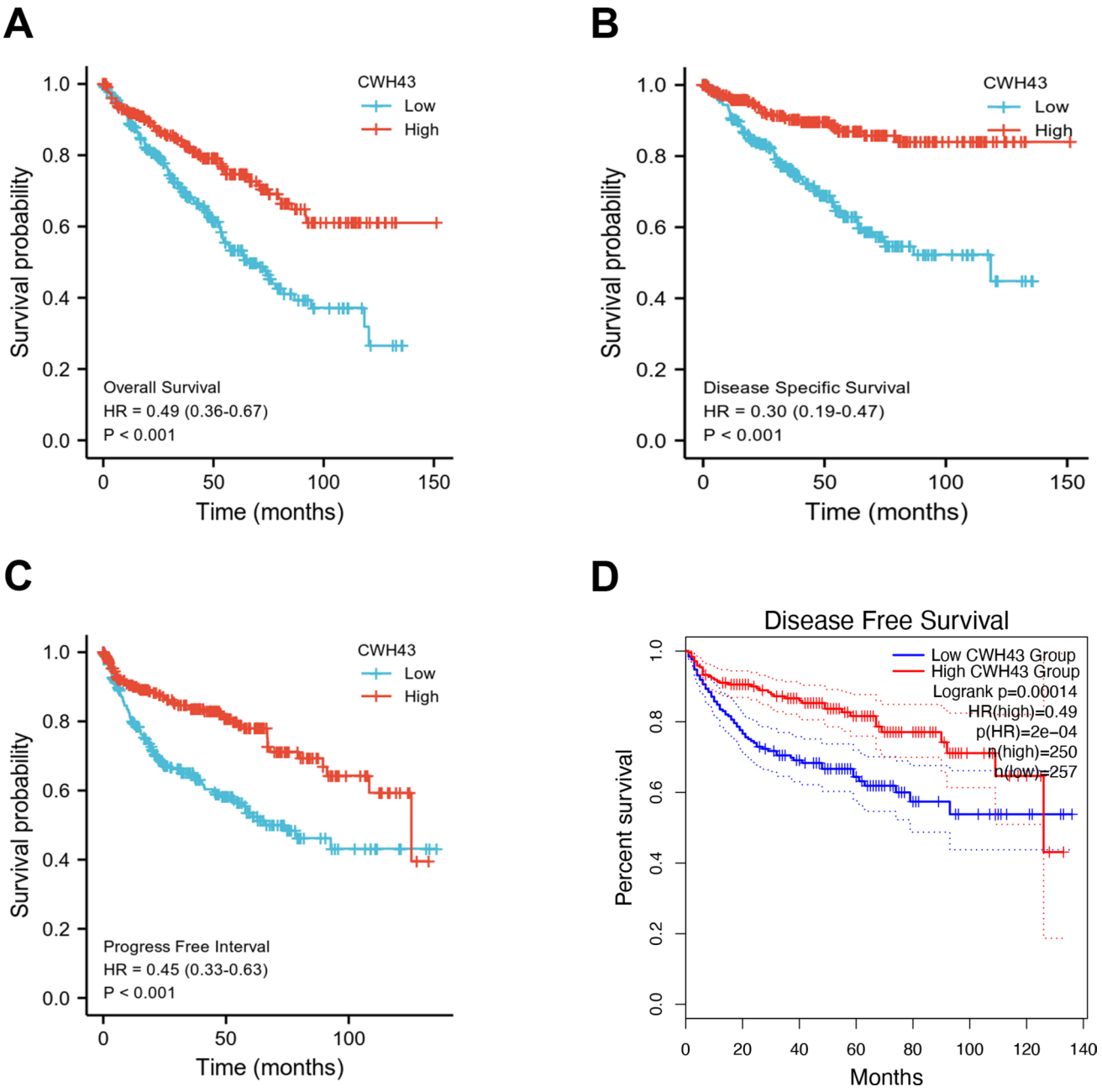

Fig. 3 Kaplan–Meier Survival Curves Based on CWH43 Expression Levels in KIRC from the TCGA Dataset. **A** Overall survival, (**B**) Disease-specific survival, (**C**) Progression-free interval, (**D**) Disease-free survival

using Cox regression, which identified age > 60 years (p = 0.028), presence of metastasis (M1) (p < 0.001), and high CWH43 expression (p = 0.013) as independent prognostic factors for OS (Table 3).

Additionally, Cox univariate regression models based on DSS and PFI data confirmed CWH43 expression as an independent prognostic factor for both DSS (p = 0.038) and PFI (p = 0.026) in ccRCC patients (Supplementary Fig. 2). This comprehensive analysis underscores the critical role of CWH43 expression in the prognostic landscape of ccRCC, highlighting its potential as a biomarker for predicting patient outcomes.

Table 3 The univariate and multivariable survival analysis of CWH43 expression in ccRCC

CpG	HR	p-value
1 stExon;5″UTR-Island-cg04005707	1.54	0.028
TSS1500-N_Shore-cg11935592	0.559	0.0082
TSS1500-Island-cg08529049	2.64	0.00023
TSS1500-Island-cg22826333	0.431	6.3e-05
TSS1500-Island-cg25484904	2.354	0.00073
TSS200-Island-cg22930650	0.525	0.0022
TSS200-Island-cg18280362	1.596	0.029
TSS200-Island-cg24534566	2.508	1e-04
TSS200-Island-cg13693941	0.764	0.17
Body-S_Shelf-cg24060908	0.397	2.5e-05
Body-Island-cg25316310	1.664	0.038
Body-S_Shore-cg03170472	1.65	0.013

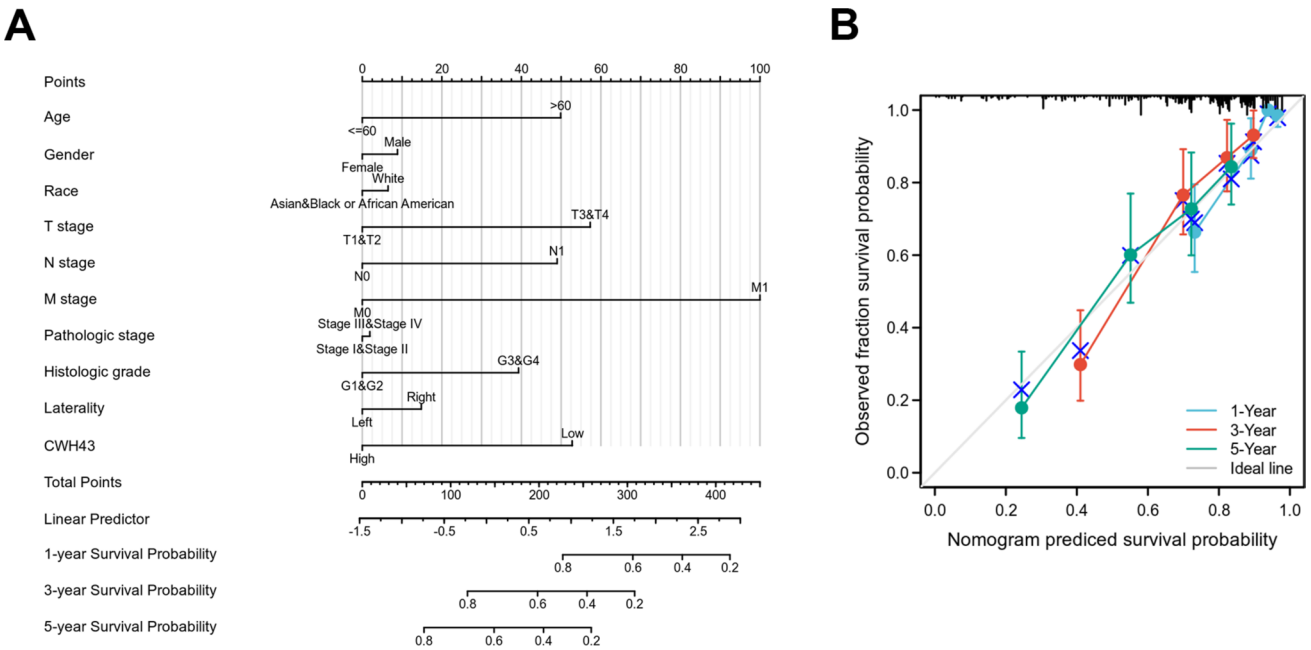

Fig. 4 Prognostic Nomogram and Calibration for ccRCC. **A** Nomogram predicting 1, 3, and 5 year overall survival probabilities for ccRCC patients. **B** Calibration plots verifying the accuracy of the nomogram predictions for 1, 3, and 5 year overall survival in ccRCC patients

3.4 Development and validation of a prognostic nomogram incorporating CWH43

A nomogram was developed that includes key prognostic factors such as age, gender, race, TNM stage, pathological stage, histologic grade, and laterality to quantitatively predict survival probabilities in patients with ccRCC (Fig. 4A). The calibration of this nomogram for predicting 1-, 3-, and 5-year survival rates demonstrated a Concordance index of 0.771, indicating strong correlation between the predicted outcomes and actual observations (Fig. 4B).

3.5 Analysis of CWH43 promoter methylation in relation to clinicopathological characteristics of renal clear cell carcinoma

DNA methylation, a chemical modification that affects gene expression without changing the DNA sequence, plays a pivotal role in gene regulation. We analyzed the methylation levels of the CWH43 promoter in renal clear cell carcinoma by utilizing the UALCAN database. Our findings indicate that the methylation level of the CWH43 promoter was substantially

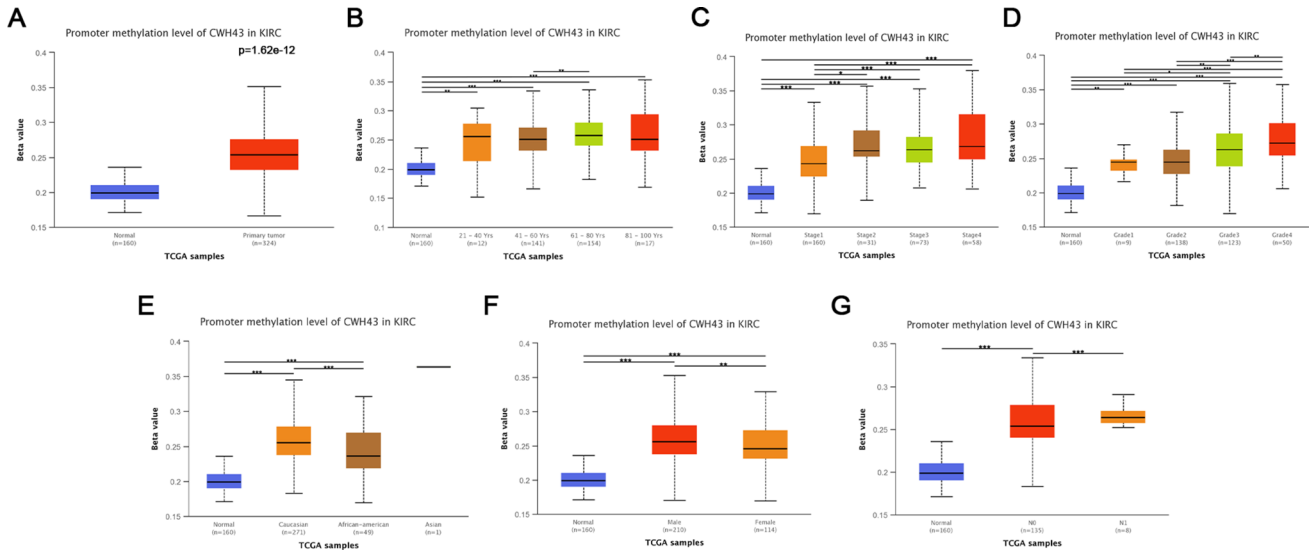

Fig. 5 Analysis of CWH43 Methylation and Its Association with Clinical Characteristics in ccRCC Patients. Methylation levels of CWH43 are analyzed by (**A**) type of sample, (**B**) age of patients, (**C**) stage of individual tumors, (**D**) grade of tumors, (**E**) race of patients, (**F**) gender of patients, and (**G**) status of nodal metastasis

higher in tumor tissues compared to normal renal tissues (p = 1.62e-12) (Fig. 5A). Subsequent subgroup analysis based on clinicopathological characteristics such as age, race, gender, cancer stage, tumor grade, and lymph node involvement revealed varying patterns of methylation. The analysis showed an increase in methylation levels correlating with advancing age, cancer stage, and tumor grade (Fig. 5B–D). Furthermore, methylation levels were found to be elevated in Caucasian and African-American patients compared to other groups, and males exhibited higher methylation than females (Fig. 5E, F). Additionally, tumors with lymph node metastasis showed increased promoter methylation compared to those without metastasis (Fig. 5G). This comprehensive assessment underscores the significance of CWH43 promoter methylation as a biomarker in the pathogenesis and progression of renal clear cell carcinoma.

3.6 Impact of CWH43 promoter methylation on prognosis in renal clear cell carcinoma

We further explored the prognostic significance of CWH43 promoter methylation in patients with ccRCC using the MethSurv tool to analyze individual CpG sites. The analysis identified 12 methylated CpG sites, particularly highlighting cg11935592 and cg24060908 for their high methylation levels (Supplementary Fig. 3 A). We assessed the relationship between CWH43 expression and the methylation status of these 12 CpG sites, revealing a negative correlation between methylation levels and CWH43 expression (Supplementary Fig. 3B).

Further investigations showed that the methylation status of 11 out of these 12 CpG sites significantly influenced prognosis, with sites cg03170472, cg11935592, cg24060908, cg22930650, cg18280362, cg08529049, cg04005707, cg24534566, cg25484904, cg22826333, and cg25316310 all associated with survival outcomes ($p < 0.05$) (Table 4). Conversely, one site, cg13693941, did not show a significant prognostic impact (p = 0.17) (Fig. 6L).

The analysis of survival data revealed divergent patterns: lower methylation levels at CpG sites cg03170472, cg04005707, cg08529049, cg18280362, cg24534566, cg25316310, and cg25484904 were associated with improved overall survival (Fig. 6A–G). Interestingly, higher methylation levels at other sites—cg11935592, cg22826333, cg22930650, cg24060908—correlated with better survival outcomes (Fig. 6H–K). These findings underscore the complex role of CWH43 promoter methylation in the prognosis of ccRCC, suggesting variable effects depending on specific CpG sites within the promoter region.

3.7 Impact of CWH43 genetic alterations on prognosis in ccRCC patients

We utilized the cBioPortal to assess how alterations in the CWH43 gene affect the prognosis of patients with ccRCC. Our findings revealed that alterations in the CWH43 gene were present in 1.1% of the sequenced cases (Fig. 7A), with mutations constituting the predominant type of genetic alteration. Additionally, amplifications of the CWH43 gene were

Table 4 Effect of CWH43 promoter methylation on prognosis in ccRCC

Cell type	Gene marker	None		Purity		Tumor		Normal	
		Cor	P	Cor	P	R	P	R	P
B cell	CD19	− 0.199	***	− 0.164	***	− 0.024	0.58	− 0.23	*
	CD20 (KRT20)	− 0.051	0.235	− 0.042	0.371	− 0.0085	0.85	− 0.034	0.780
	CD38	− 0.239	***	− 0.249	***	− 0.028	0.53	− 0.21	0.077
CD8 +T cell	CD8 A	− 0.228	***	− 0.23	***	− 0.058	0.19	− 0.39	***
	CD8B	− 0.205	***	− 0.197	***	− 0.062	0.16	− 0.22	0.067
Tfh	BCL6	− 0.069	0.113	− 0.081	0.084	− 0.1	*	− 0.018	0.880
	ICOS	− 0.255	***	− 0.255	***	− 0.06	0.17	− 0.29	*
	CXCR5	− 0.258	***	− 0.224	***	− 0.11	*	− 0.22	0.061
Th1	T− bet (TBX21)	− 0.006	0.896	0.023	0.615	− 0.12	**	− 0.37	**
	STAT4	− 0.192	***	− 0.183	***	− 0.19	***	− 0.35	**
	IL12RB2	− 0.003	0.945	0.017	0.711	− 0.025	0.57	0.048	0.690
	WSX1 (IL27RA)	− 0.073	0.093	− 0.031	0.505	− 0.16	***	− 0.11	0.350
	STAT1	− 0.172	***	− 0.181	***	− 0.16	***	− 0.11	0.350
	IFN-γ (IFNG)	− 0.265	***	− 0.27	***	− 0.035	0.42	− 0.17	0.160
	TNF-α(TNF)	− 0.027	0.530	− 0.002	0.968	− 0.058	0.19	− 0.11	0.340
Th2	GATA3	0.072	0.099	0.092	0.049	0.033	0.45	0.48	***
	CCR3	− 0.139	**	− 0.138	**	− 0.041	0.35	− 0.27	*
	STAT6	0.142	**	0.131	**	− 0.072	0.099	− 0.051	0.670
	STAT5 A	− 0.204	***	− 0.187	***	− 0.089	*	− 0.18	0.120
Th9	TGFBR2	0.32	***	0.318	***	− 0.045	0.3	− 0.02	0.860
	IRF4	− 0.275	***	− 0.267	***	− 0.039	0.37	− 0.2	0.089
	PU.1 (SPI1)	− 0.287	***	− 0.289	***	− 0.094	*	− 0.42	***
Th17	STAT3	0.071	0.100	0.085	0.069	− 0.12	**	0.17	0.150
	IL-21R	− 0.204	***	− 0.182	***	− 0.059	0.17	− 0.31	**
	IL-23R	− 0.114	**	− 0.089	0.056	− 0.053	0.23	− 0.29	*
	IL-17 A	− 0.07	0.106	− 0.042	0.364	− 0.044	0.32	− 0.0043	0.970
Th22	CCR10	− 0.042	0.338	0.014	0.764	− 0.083	0.056	0.07	0.560
	AHR	0.133	**	0.132	**	− 0.097	*	− 0.2	0.091
Treg	FOXP3	− 0.359	***	− 0.359	***	− 0.11	**	− 0.2	0.084
	CD25 (IL2RA)	− 0.148	***	− 0.146	**	− 0.0098	0.82	− 0.35	**
	CCR8	− 0.259	***	− 0.262	***	− 0.084	0.054	− 0.26	*
T cell exhaustion	PD-1 (PDCD1)	− 0.296	***	− 0.305	***	− 0.058	0.18	− 0.29	*
	CTLA4	− 0.31	***	− 0.323	***	− 0.074	0.089	− 0.29	*
	LAG3	− 0.317	***	− 0.317	***	− 0.018	0.68	− 0.29	*
	TIM-3 (HAVCR2)	− 0.092	*	− 0.097	*	− 0.085	0.053	− 0.17	0.160
Macrophage	CD68	− 0.25	***	− 0.261	***	− 0.062	0.16	− 0.39	***
	CD11b (ITGAM)	− 0.211	***	− 0.205	***	− 0.045	0.3	− 0.4	***
M1	INOS (NOS2)	0.223	***	0.254	***	− 0.039	0.37	0.099	0.410
	IRF5	− 0.224	***	− 0.214	***	− 0.14	**	0.11	0.370
	COX2 (PTGS2)	0.057	0.191	0.062	0.187	− 0.012	0.78	− 0.06	0.620
M2	CD163	− 0.132	**	− 0.147	**	− 0.06	0.17	− 0.38	***
	ARG1	0.056	0.197	0.042	0.370	0.026	0.55	− 0.27	*
	MRC1	0.188	***	0.196	***	− 0.056	0.2	− 0.23	*
	MS4 A4 A	− 0.151	***	− 0.157	***	− 0.092	*	− 0.39	***
TAM	CCL2	0.051	0.237	0.103	*	− 0.083	0.057	− 0.029	0.810
	CD80	− 0.26	***	− 0.268	***	− 0.012	0.78	− 0.22	0.068
	CD86	− 0.252	***	− 0.266	***	− 0.083	0.058	− 0.36	**
	CCR5	− 0.235	***	− 0.241	***	− 0.072	0.098	− 0.38	***

Table 4 (continued)

Cell type	Gene marker	None		Purity		Tumor		Normal	
		Cor	P	Cor	P	R	P	R	P
Monocyte	CD14	− 0.208	***	− 0.195	***	− 0.11	*	− 0.39	***
	CD16 (FCGR3B)	− 0.022	0.607	− 0.052	0.268	− 0.062	0.16	− 0.26	*
	CD115 (CSF1R)	− 0.2	***	− 0.199	***	− 0.11	*	− 0.4	***
Neutrophil	CD66b (CEACAM8)	0.08	0.066	0.073	0.117	− 0.021	0.63	− 0.12	0.320
	CD15 (FUT4)	− 0.025	0.561	− 0.021	0.659	− 0.13	**	− 0.16	0.190
	CD11b (ITGAM)	− 0.211	***	− 0.205	***	− 0.045	0.3	− 0.4	***
Natural killer cell	XCL1	− 0.326	***	− 0.306	***	− 0.11	**	− 0.19	0.110
	CD7	− 0.268	***	− 0.26	***	− 0.023	0.6	− 0.42	***
	KIR3DL1	0.118	**	0.137	**	− 0.095	*	− 0.18	0.140
Dendritic cell	CD1 C (BDCA-1)	0.073	0.091	0.097	*	− 0.076	0.083	− 0.27	*
	CD141 (THBD)	0.08	0.065	0.131	**	− 0.11	*	− 0.09	0.450
	CD11c (ITGAX)	− 0.257	***	− 0.261	***	0.03	0.49	− 0.33	**

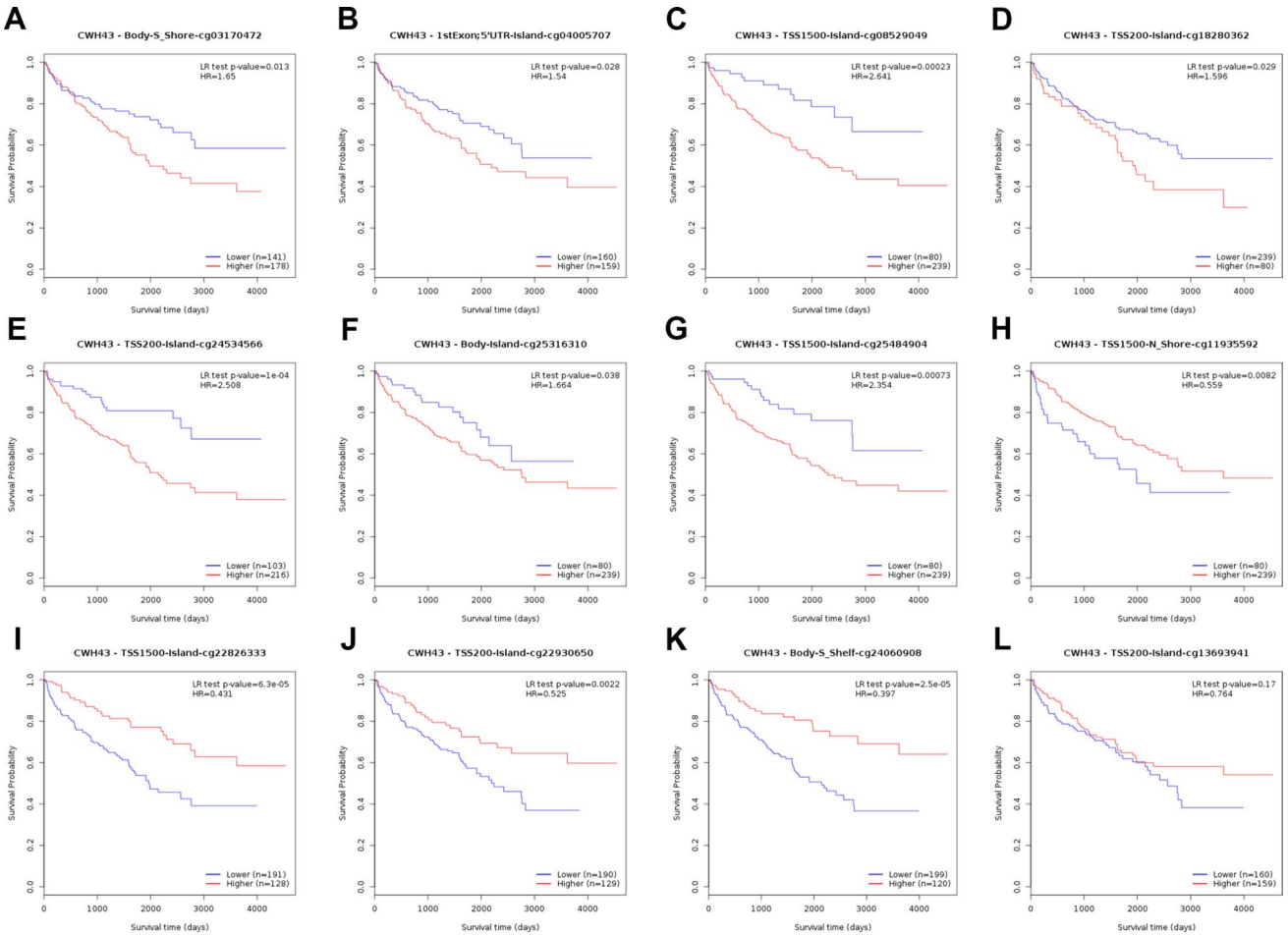

Fig. 6 Survival Outcomes Based on CWH43 Promoter Methylation at Specific CpG Sites in ccRCC. Kaplan–Meier curves illustrating overall survival (OS) for low and high methylation at CpG sites: (**A**) cg03170472, (**B**) cg04005707, (C) cg08529049, (**D**) cg18280362, (**E**) cg24534566, (**F**) cg25316310, (**G**) cg25484904, (**H**) cg11935592, (**I**) cg22826333, (**J**) cg22930650, (**K**) cg24060908, and (**L**) cg13693941

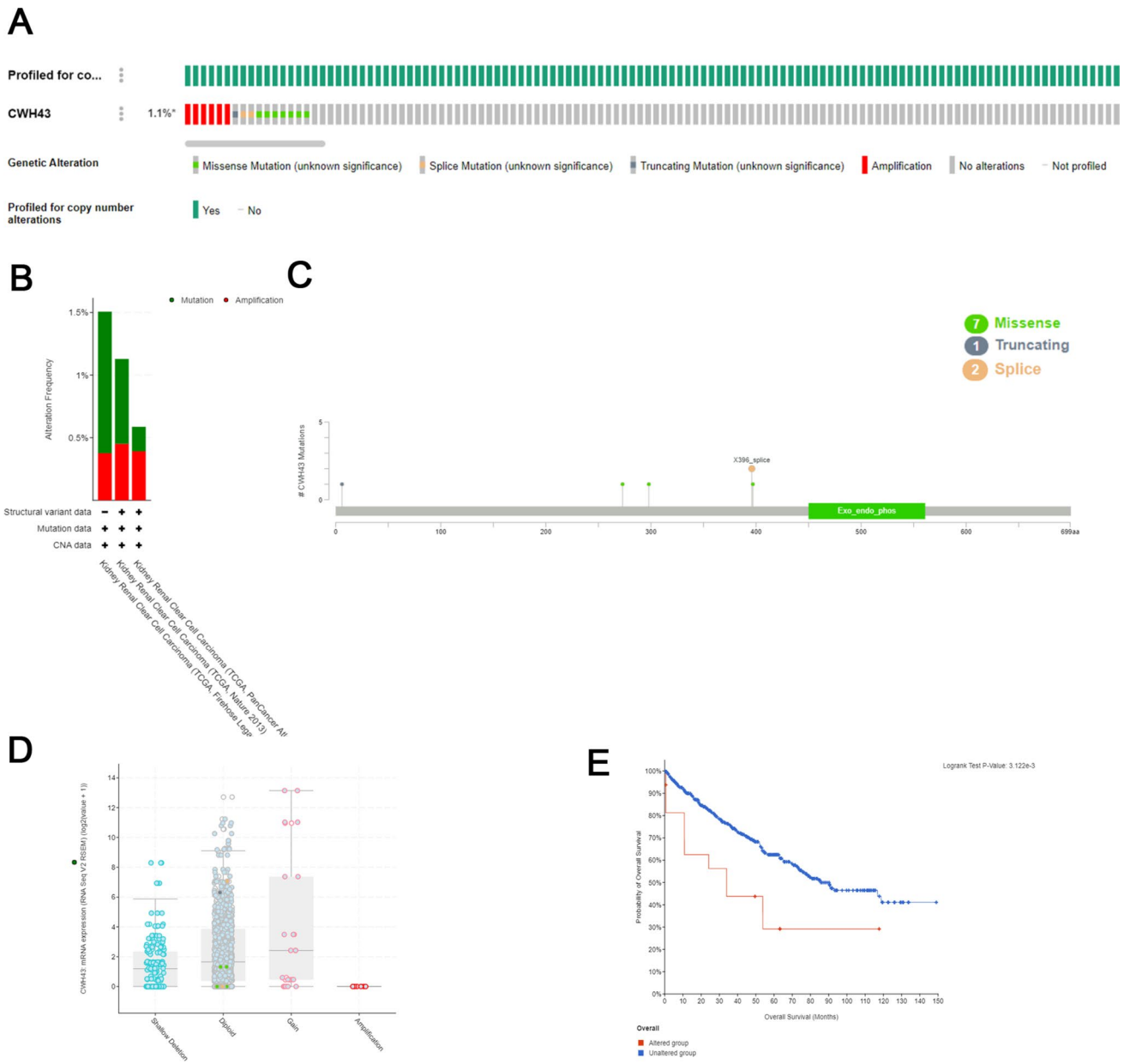

Fig. 7 Relationship Between Genetic Alterations in CWH43 and Prognosis in ccRCC. **A** OncoPrint visualizing CWH43 alterations. Various genetic alterations are depicted in distinct colors. **B** Analysis of mutation frequency and (**C**) mutation sites via cBioPortal. **D** Expression levels across different CWH43 copy number variations (CNV) groups, noting a significant expression increase in the CWH43 gain group. **E** Kaplan–Meier plots assessing the impact of CWH43 gene alterations on overall survival

observed in some instances of renal clear cell carcinoma (Fig. 7B). A detailed examination of the mutations identified three missense mutations, one truncating mutation, and one splice site mutation (Fig. 7C).

Further analysis indicated that a gain in CWH43 led to its increased expression. Specifically, CWH43 expression levels were higher in both diploid and gain status groups compared to the shallow deletion group (Fig. 7D). Lastly, we evaluated the prognostic implications of CWH43 gene alterations in ccRCC patients. The analysis demonstrated that patients with alterations in the CWH43 gene exhibited poorer overall survival compared to those without such alterations (Fig. 7E) ($p = 3.122e\text{-}3$), highlighting the significance of genetic changes in CWH43 as an indicator of adverse outcomes in ccRCC.

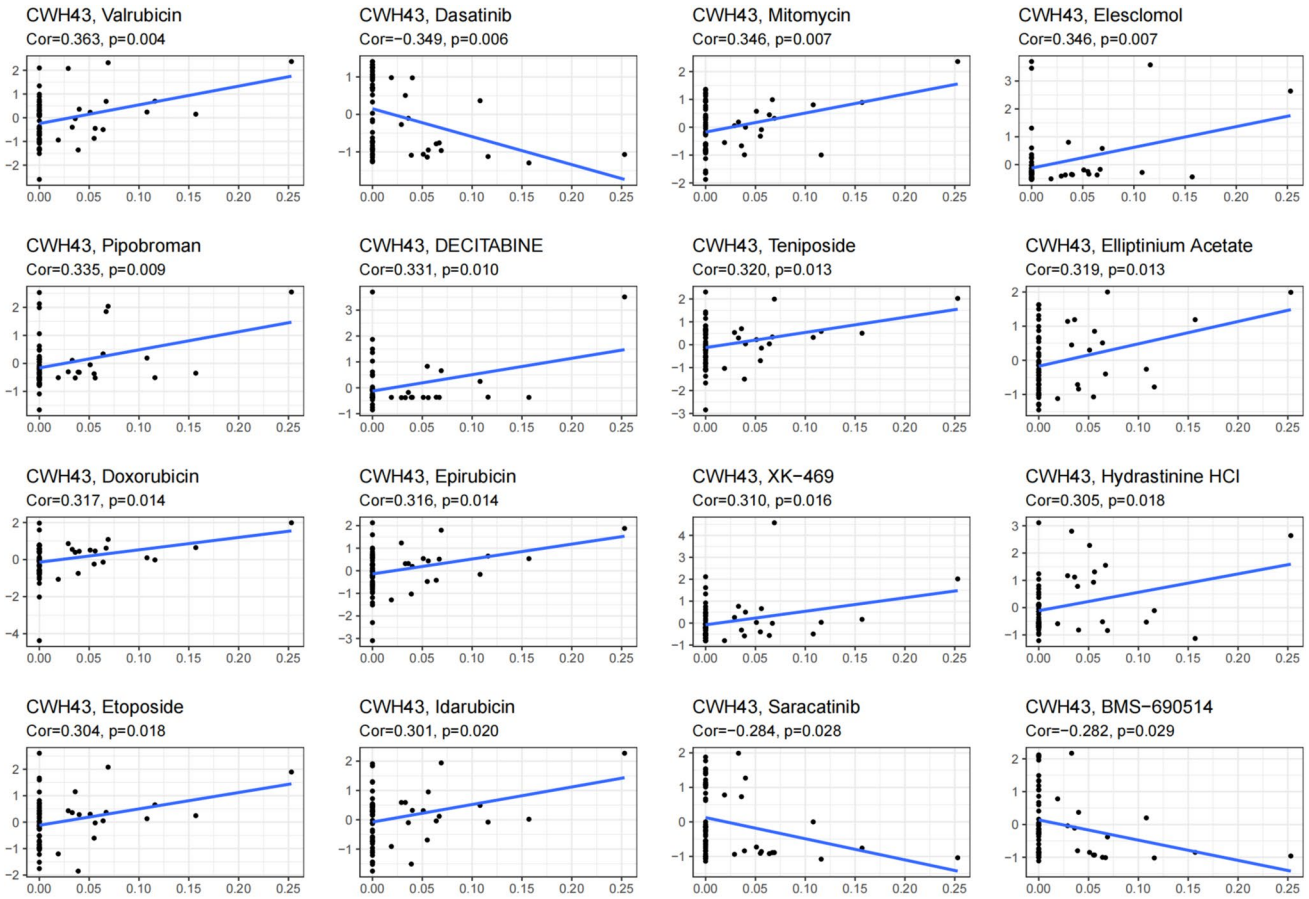

Fig. 8 Correlation Between CWH43 Expression and Drug Sensitivity in ccRCC. This figure plots CWH43 gene expression against the sensitivity to various anticancer drugs

3.8 Association of CWH43 gene expression with anticancer drug sensitivity

We investigated the relationship between CWH43 gene expression and sensitivity to anticancer drugs using the CellMiner database. Our analysis identified 27 anticancer drugs whose sensitivities exhibited significant correlations with CWH43 expression. Of these, the sensitivity to 22 drugs showed a positive correlation with higher CWH43 expression, whereas sensitivity to 5 drugs was negatively correlated.

Figure 8 presents the correlations for the top 16 drugs. Notably, CWH43 expression was significantly negatively correlated with the sensitivity to Dasatinib, Saracatinib, and BMS-690514. Conversely, a positive correlation was found between CWH43 expression and the sensitivity to several other drugs, including Valrubicin, Mitomycin, Elesclomol, Pipobroman, Decitabine, Teniposide, Elliptinium Acetate, Doxorubicin, Epirubicin, XK-469, Hydrastinine HCl, Etoposide, and Idarubicin. For a comprehensive overview of all findings, refer to Supplementary Table 1. These results underscore the potential of CWH43 expression as a biomarker for predicting the efficacy of specific anticancer therapies in clinical settings.

3.9 CWH43 and its role in forming an inflammatory tumor microenvironment in ccRCC

Investigations into the role of CWH43 in the tumor microenvironment (TME) of ccRCC revealed a notable negative correlation between CWH43 expression and a wide array of immunomodulators (Fig. 9A). Specifically, in the group with low CWH43 expression, there was an observed increase in most MHC molecules, indicating enhanced antigen presentation and processing. Additionally, elevated expression of key chemokines such as CXCL9, CXCL10, and CCR3 in this group facilitated the recruitment of CD8 + T cells to the TME. Other chemokines including CCL1, CCL4, CCL5, CCL15, CCL18, CCL19, CCL22, CCL23, and associated receptors such as CCR1, CCR2, CCR3, CCR4, CCR5, CCR7, CXCR3, CXCR4, CXCR5, CXCR6 were

Fig. 9 Influence of CWH43 Expression on Tumor Microenvironment (TME) in ccRCC. **A** Expression differences in 122 immunomodulators between high and low CWH43 expression groups. **B** Variations in cancer-immune cycle steps between groups. Differences in (**C**) immune score, (**D**) stromal score, (**E**) ESTIMATE score, (**F**) tumor purity, (**G**) interactions with infiltrating immune cells, and (H) expression of immune checkpoints between groups. Statistical significance is noted as *p < 0.05; **p < 0.01; ***p < 0.001

found to be negatively correlated with CWH43 expression. These chemokines and receptors are crucial for the mobilization of effector tumor-infiltrating immune cells (TIICs), including CD8 + T cells, Th17 cells, and antigen-presenting cells.

Given the complex and multifunctional nature of the chemokine system, the relationship between individual chemokines and CWH43 does not fully capture the overall immune role of CWH43 in the TME. The functionality of the chemokine system, alongside other immune modulators, directly manifests through the cancer-immune cycle. In the CWH43 low expression group, we observed upregulation in most steps of this cycle, including the release of cancer cell antigens, expression of these antigens, priming and activation of immune responses, transport of immune cells to the tumor, infiltration of these cells into the tumor, and recognition of cancer cells by T cells (Fig. 9B,C).

Enhanced activity in these steps likely increases the infiltration of effector TIICs, thereby altering the composition of the TME. This was further analyzed using the ESTIMATE tool, where the results indicated higher immune scores (p = 5.4e-09) (Fig. 9C-E), and a lower tumor purity in the low CWH43 expression group, suggesting a robust immune presence (Fig. 9F).

A systematic analysis of immune cell types within tumors, comparing the high and low CWH43 expression groups within the TCGA dataset, revealed differing levels of various immune cells. Notably, the high CWH43 expression group exhibited increased levels of native B cells, macrophage M0, macrophage M1, and resting mast cells, while the low expression group showed higher levels of follicular helper T cells, regulatory T cells (Tregs), resting NK cells, and resting dendritic cells (Fig. 9G).

Further analyses explored the correlation between CWH43 expression and immune cell markers across various immune cell types, using the TIMER and GEPIA databases. Significant correlations were observed between CWH43 expression and the infiltration levels of diverse immune cells, including Tfh, Th1, Th2, Th9, Th22, Treg cells, M1/M2 macrophages, monocytes, and natural killer cells (Table 5).

The influence of CWH43 on immune checkpoints was also examined, revealing significant upregulation of 27 immune checkpoint genes and downregulation of seven in the low expression group of CWH43 compared to the high expression group (Fig. 9H). This suggests that CWH43 may regulate the immune landscape of ccRCC by modulating the expression levels of key immune checkpoint genes, highlighting its potential role in immune evasion mechanisms within the TME.

3.10 Evaluating CWH43's interaction with immunotherapy mechanisms

CWH43 displayed a predominantly negative association with the enrichment of many immunotherapy-responsive gene signatures, as evidenced by data presented in Fig. 10A. This gene was also inversely related to several critical phases within the cancer-immune cycle. These phases include the release of antigens by cancer cells (Step 1), expression of tumor antigens (Step 2), activation and priming of immune responses (Step 3), and the mobilization of immune cells towards the tumor site (Step 4). The latter encompasses the recruitment of T cells, CD4 cells, CD8 T cells, Th1 cells, Th22 cells, macrophages, monocytes, neutrophils, NK cells, Th17 cells, B cells, Th2 cells, Treg cells, and MDSCs. Furthermore, CWH43 negatively influenced the infiltration of these immune cells into tumors (Step 5), their ability to recognize cancer cells (Step 6), and ultimately, their capacity to eliminate cancer cells (Step 7) (Fig. 10B).

In addition, we explored the relationship between CWH43 expression and predicted responses to immune checkpoint blockade (ICB). CWH43 showed a negative correlation with certain positive immunotherapy signals such as the Systemic lupus erythematosus and p53 signaling pathways, alongside MicroRNAs in cancer. Conversely, it positively correlated with pathways including Pyrimidine metabolism, the Cytokine-cytokine receptor interaction, Cell cycle progression, oocyte meiosis, viral carcinogenesis, base excision repair, spliceosome activity, and RNA degradation processes (Fig. 10C).

These insights highlight CWH43's substantial role in modulating the immune landscape within ccRCC, impacting both the efficacy of immunotherapeutic approaches and the broader cancer-immune cycle. This intricate involvement suggests that CWH43 may serve as a valuable biomarker for tailoring immunotherapy strategies in clinical oncology.

3.11 Exploring the molecular dynamics of CWH43 in ccRCC through functional enrichment analysis

To decode the molecular basis of CWH43's involvement in clear cell renal cell carcinoma (ccRCC), we leveraged the "DESeq2" R package to identify differentially expressed genes (DEGs) between groups exhibiting high and low expression

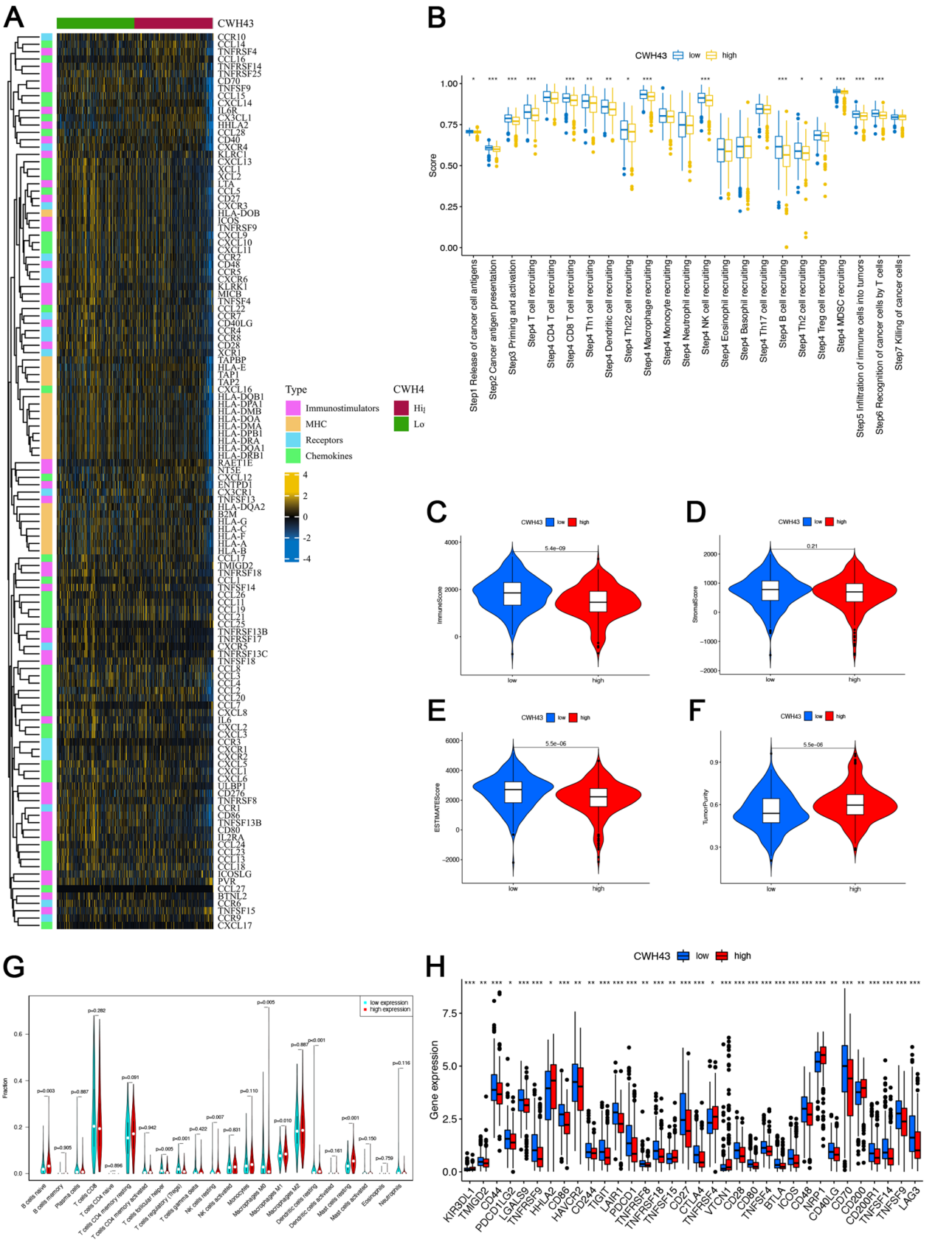
A
CWH43
Type
Immunostimulators
MHC
Receptors
Chemokines
CWH4
Hi
Lo
B
CWH43 low high
Score
Step1 Release of cancer cell antigens
Step2 Cancer antigen presentation
Step3 Priming and activation
Step4 T cell recruiting
Step4 CD4 T cell recruiting
Step4 CD8 T cell recruiting
Step4 Th1 cell recruiting
Step4 Dendritic cell recruiting
Step4 Th22 cell recruiting
Step4 Macrophage recruiting
Step4 Monocyte recruiting
Step4 Neutrophil recruiting
Step4 NK cell recruiting
Step4 Eosinophil recruiting
Step4 Basophil recruiting
Step4 Th17 cell recruiting
Step4 B cell recruiting
Step4 Th2 cell recruiting
Step4 Treg cell recruiting
Step4 MDSC recruiting
Step5 Infiltration of immune cells into tumors
Step6 Recognition of cancer cells by T cells
Step7 Killing of cancer cells
C
CWH43 low high
5.4e-09
ImmuneScore
D
CWH43 low high
0.21
StromalScore
E
CWH43 low high
5.5e-06
ESTIMATEScore
F
CWH43 low high
5.5e-06
TumorPurity
G
low expression
high expression
Fraction
B cells naive
B cells memory
Plasma cells
T cells CD8
T cells CD4 naive
T cells CD4 memory resting
T cells CD4 memory activated
T cells follicular helper
T cells regulatory (Tregs)
T cells gamma delta
NK cells resting
NK cells activated
Monocytes
Macrophages M0
Macrophages M1
Macrophages M2
Dendritic cells resting
Dendritic cells activated
Mast cells resting
Mast cells activated
Eosinophils
Neutrophils
H
CWH43 low high
Gene expression
KIR3DL1
TMIGD2
CD44
PDCD1LG2
LGALS9
TNFRSF9
HHLA2
CD86
HAVCR2
CD244
TIGIT
LAIR1
PDCD1
TNFRSF8
TNFRSF18
TNFSF15
CD27
CTLA4
TNFRSF4
VTCN1
CD28
CD80
TNFSF4
BTLA
ICOS
CD48
NRP1
CD40LG
CD70
CD200
CD200R1
TNFSF14
TNFSF9
LAG3

Table 5 Correlation analysis between CWH43 and markers of immune cells in TIMER and GEPIA

Cell type	Gene marker	None		Purity		Tumor		Normal	
		Cor	*P*	*Cor*	*P*	*R*	*P*	*R*	*P*
B cell	CD19	− 0.199	***	− 0.164	***	− 0.024	0.58	− 0.23	*
	CD20 (KRT20)	− 0.051	0.235	− 0.042	0.371	− 0.0085	0.85	− 0.034	0.780
	CD38	− 0.239	***	− 0.249	***	− 0.028	0.53	− 0.21	0.077
CD8 +T cell	CD8 A	− 0.228	***	− 0.23	***	− 0.058	0.19	− 0.39	***
	CD8B	− 0.205	***	− 0.197	***	− 0.062	0.16	− 0.22	0.067
Tfh	BCL6	− 0.069	0.113	− 0.081	0.084	− 0.1	*	− 0.018	0.880
	ICOS	− 0.255	***	− 0.255	***	− 0.06	0.17	− 0.29	*
	CXCR5	− 0.258	***	− 0.224	***	− 0.11	*	− 0.22	0.061
Th1	T-bet (TBX21)	− 0.006	0.896	0.023	0.615	− 0.12	**	− 0.37	**
	STAT4	− 0.192	***	− 0.183	***	− 0.19	***	− 0.35	**
	IL12RB2	− 0.003	0.945	0.017	0.711	− 0.025	0.57	0.048	0.690
	WSX1 (IL27RA)	− 0.073	0.093	− 0.031	0.505	− 0.16	***	− 0.11	0.350
	STAT1	− 0.172	***	− 0.181	***	− 0.16	***	− 0.11	0.350
	IFN-γ (IFNG)	− 0.265	***	− 0.27	***	− 0.035	0.42	− 0.17	0.160
	TNF-α (TNF)	− 0.027	0.530	− 0.002	0.968	− 0.058	0.19	− 0.11	0.340
Th2	GATA3	0.072	0.099	0.092	0.049	0.033	0.45	0.48	***
	CCR3	− 0.139	**	− 0.138	**	− 0.041	0.35	− 0.27	*
	STAT6	0.142	**	0.131	**	− 0.072	0.099	− 0.051	0.670
	STAT5 A	− 0.204	***	− 0.187	***	− 0.089	*	− 0.18	0.120
Th9	TGFBR2	0.32	***	0.318	***	− 0.045	0.3	− 0.02	0.860
	IRF4	− 0.275	***	− 0.267	***	− 0.039	0.37	− 0.2	0.089
	PU.1 (SPI1)	− 0.287	***	− 0.289	***	− 0.094	*	− 0.42	***
Th17	STAT3	0.071	0.100	0.085	0.069	− 0.12	**	0.17	0.150
	IL-21R	− 0.204	***	− 0.182	***	− 0.059	0.17	− 0.31	**
	IL-23R	− 0.114	**	− 0.089	0.056	− 0.053	0.23	− 0.29	*
	IL-17 A	− 0.07	0.106	− 0.042	0.364	− 0.044	0.32	− 0.0043	0.970
Th22	CCR10	− 0.042	0.338	0.014	0.764	− 0.083	0.056	0.07	0.560
	AHR	0.133	**	0.132	**	− 0.097	*	− 0.2	0.091
Treg	FOXP3	− 0.359	***	− 0.359	***	− 0.11	**	− 0.2	0.084
	CD25 (IL2RA)	− 0.148	***	− 0.146	**	− 0.0098	0.82	− 0.35	**
	CCR8	− 0.259	***	− 0.262	***	− 0.084	0.054	− 0.26	*
T cell exhaustion	PD-1 (PDCD1)	− 0.296	***	− 0.305	***	− 0.058	0.18	− 0.29	*
	CTLA4	− 0.31	***	− 0.323	***	− 0.074	0.089	− 0.29	*
	LAG3	− 0.317	***	− 0.317	***	− 0.018	0.68	− 0.29	*
	TIM-3 (HAVCR2)	− 0.092	*	− 0.097	*	− 0.085	0.053	− 0.17	0.160
Macrophage	CD68	− 0.25	***	− 0.261	***	− 0.062	0.16	− 0.39	***
	CD11b (ITGAM)	− 0.211	***	− 0.205	***	− 0.045	0.3	− 0.4	***
M1	INOS (NOS2)	0.223	***	0.254	***	− 0.039	0.37	0.099	0.410
	IRF5	− 0.224	***	− 0.214	***	− 0.14	**	0.11	0.370
	COX2 (PTGS2)	0.057	0.191	0.062	0.187	− 0.012	0.78	− 0.06	0.620
M2	CD163	− 0.132	**	− 0.147	**	− 0.06	0.17	− 0.38	***
	ARG1	0.056	0.197	0.042	0.370	0.026	0.55	− 0.27	*
	MRC1	0.188	***	0.196	***	− 0.056	0.2	− 0.23	*
	MS4 A4 A	− 0.151	***	− 0.157	***	− 0.092	*	− 0.39	***
TAM	CCL2	0.051	0.237	0.103	*	− 0.083	0.057	− 0.029	0.810
	CD80	− 0.26	***	− 0.268	***	− 0.012	0.78	− 0.22	0.068
	CD86	− 0.252	***	− 0.266	***	− 0.083	0.058	− 0.36	**
	CCR5	− 0.235	***	− 0.241	***	− 0.072	0.098	− 0.38	***

Table 5 (continued)

Cell type	Gene marker	None		Purity		Tumor		Normal	
		Cor	*P*	*Cor*	*P*	*R*	*P*	*R*	*P*
Monocyte	CD14	− 0.208	***	− 0.195	***	− 0.11	*	− 0.39	***
	CD16 (FCGR3B)	− 0.022	0.607	− 0.052	0.268	− 0.062	0.16	− 0.26	*
	CD115 (CSF1R)	− 0.2	***	− 0.199	***	− 0.11	*	− 0.4	***
Neutrophil	CD66b (CEACAM8)	0.08	0.066	0.073	0.117	− 0.021	0.63	− 0.12	0.320
	CD15 (FUT4)	− 0.025	0.561	− 0.021	0.659	− 0.13	**	− 0.16	0.190
	CD11b (ITGAM)	− 0.211	***	− 0.205	***	− 0.045	0.3	− 0.4	***
Natural killer cell	XCL1	− 0.326	***	− 0.306	***	− 0.11	**	− 0.19	0.110
	CD7	− 0.268	***	− 0.26	***	− 0.023	0.6	− 0.42	***
	KIR3DL1	0.118	**	0.137	**	− 0.095	*	− 0.18	0.140
Dendritic cell	CD1 C (BDCA-1)	0.073	0.091	0.097	*	− 0.076	0.083	− 0.27	*
	CD141 (THBD)	0.08	0.065	0.131	**	− 0.11	*	− 0.09	0.450
	CD11c (ITGAX)	− 0.257	***	− 0.261	***	0.03	0.49	− 0.33	**

Tfh Follicular helper T cell, Th T helper cell, Treg Regulatory T cell, TAM Tumor-associated macrophage. None, Correlation without adjustment. Purity, Correlation adjusted by purity. Cor, R value of Spearman's correlation

*P < 0.05

**P < 0.01

***P < 0.001

of CWH43. The analysis encompassed 270 samples from the high expression group and 269 from the low expression group, resulting in the identification of 4,987 DEGs, comprising 2,776 up-regulated and 2,211 down-regulated genes, all meeting the statistical significance criteria (|log2 FC|> 1, adjusted p-value < 0.05) (Fig. 11A; Supplementary Table 2). A heat map was generated to display the top 10 up-regulated and down-regulated DEGs across these groups (Fig. 11B).

Further, to delineate the functional roles of these DEGs, Gene Ontology (GO) and Kyoto Encyclopedia of Genes and Genomes (KEGG) pathway enrichment analyses were conducted using the"clusterProfiler"package. Stringent thresholds (p.adj < 0.05 & FDR < 0.25) were applied to identify significantly enriched terms. The enrichment analysis revealed that biological processes primarily involved autophagic mechanisms, including autophagy itself and its regulation. Cellular components significantly enriched included cell-substrate junctions, substrate adherens junctions, focal adhesions, and autophagosomes. In terms of molecular function, significant enrichments were found in cell adhesion molecule binding, actin binding, and cadherin binding (Fig. 11C).

KEGG pathway analysis highlighted several critical signaling pathways impacted by these DEGs, including the PI3 K-Akt signaling pathway, MAPK signaling pathway, FoxO signaling pathway, Th17 cell differentiation, and AMPK signaling pathway (Fig. 11D). These findings offer insights into the complex regulatory networks influenced by CWH43 expression levels in ccRCC, potentially guiding targeted therapeutic strategies and deepening understanding of the disease's pathophysiology.

3.12 The role of CWH43 in autophagic processes in ccRCC

Functional enrichment analyses indicate a strong link between CWH43 expression and autophagic mechanisms within tumors, with several pathways identified as mediators of tumorigenic autophagy [33–35]. Autophagy, a critical biological process, plays a vital role in ccRCC, with deviations from normal autophagic processes closely tied to cancer progression [36]. Consequently, we investigated the relationship between CWH43 expression and autophagy in ccRCC by accessing a set of genes from the human autophagy database known to directly or indirectly influence autophagy.

Our analyses revealed a significant correlation between CWH43 expression and 27 autophagy-related genes in ccRCC. Specifically, CWH43 expression positively correlated with 14 of these genes and negatively with 9 (Fig. 12A; Supplementary Table 4). To visually depict these relationships, scatter plots were generated for the top 8 autophagy-related genes, illustrating the nature of these correlations (Figs. 12B–I).

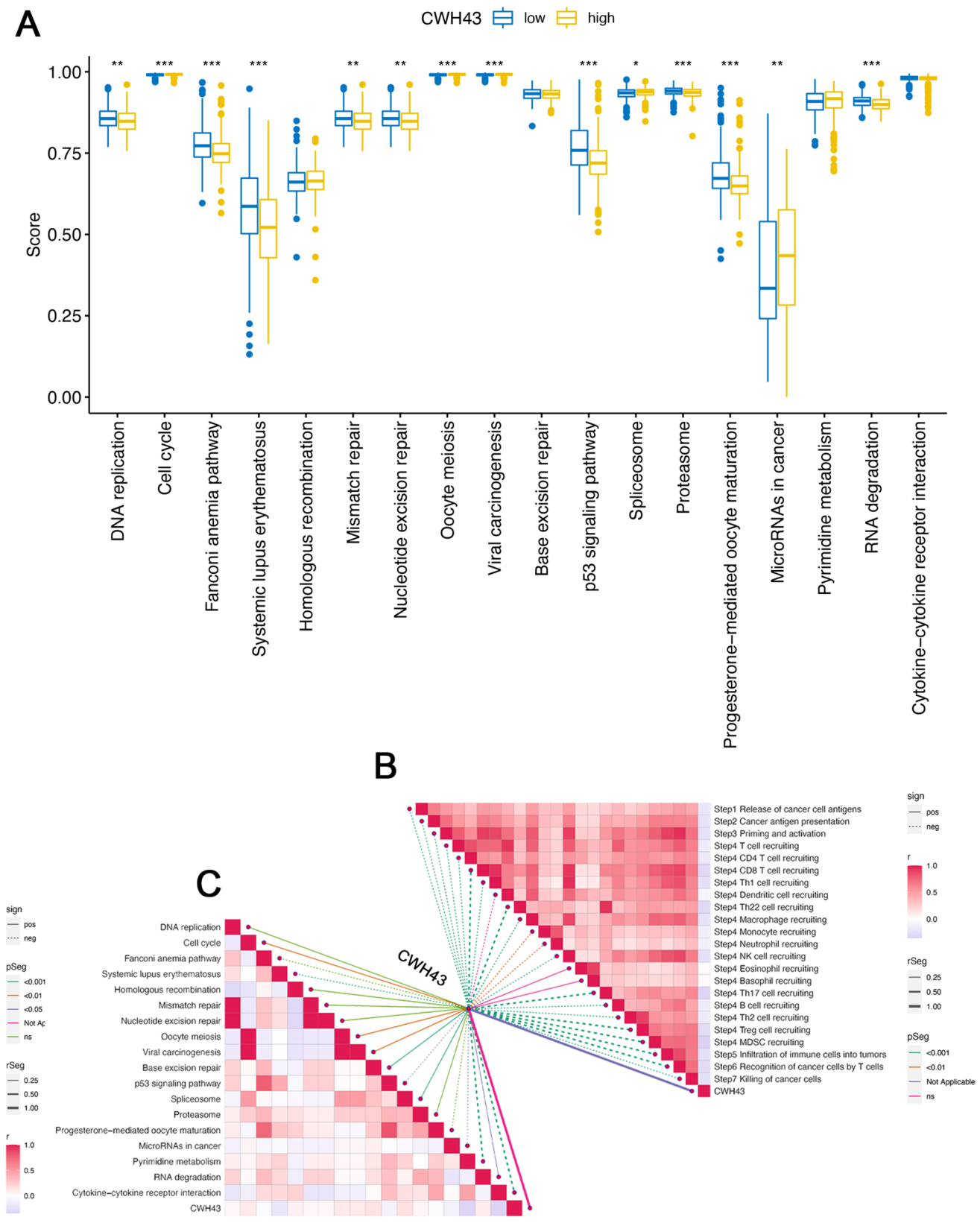

Fig. 10 CWH43's Role in Immunotherapy for ccRCC. **A** Correlation of CWH43 with clinical immunotherapy response. **B** Association of CWH43 with stages of the cancer-immune cycle. **C** Links between CWH43 and enriched pathways predictive of immunotherapy outcomes

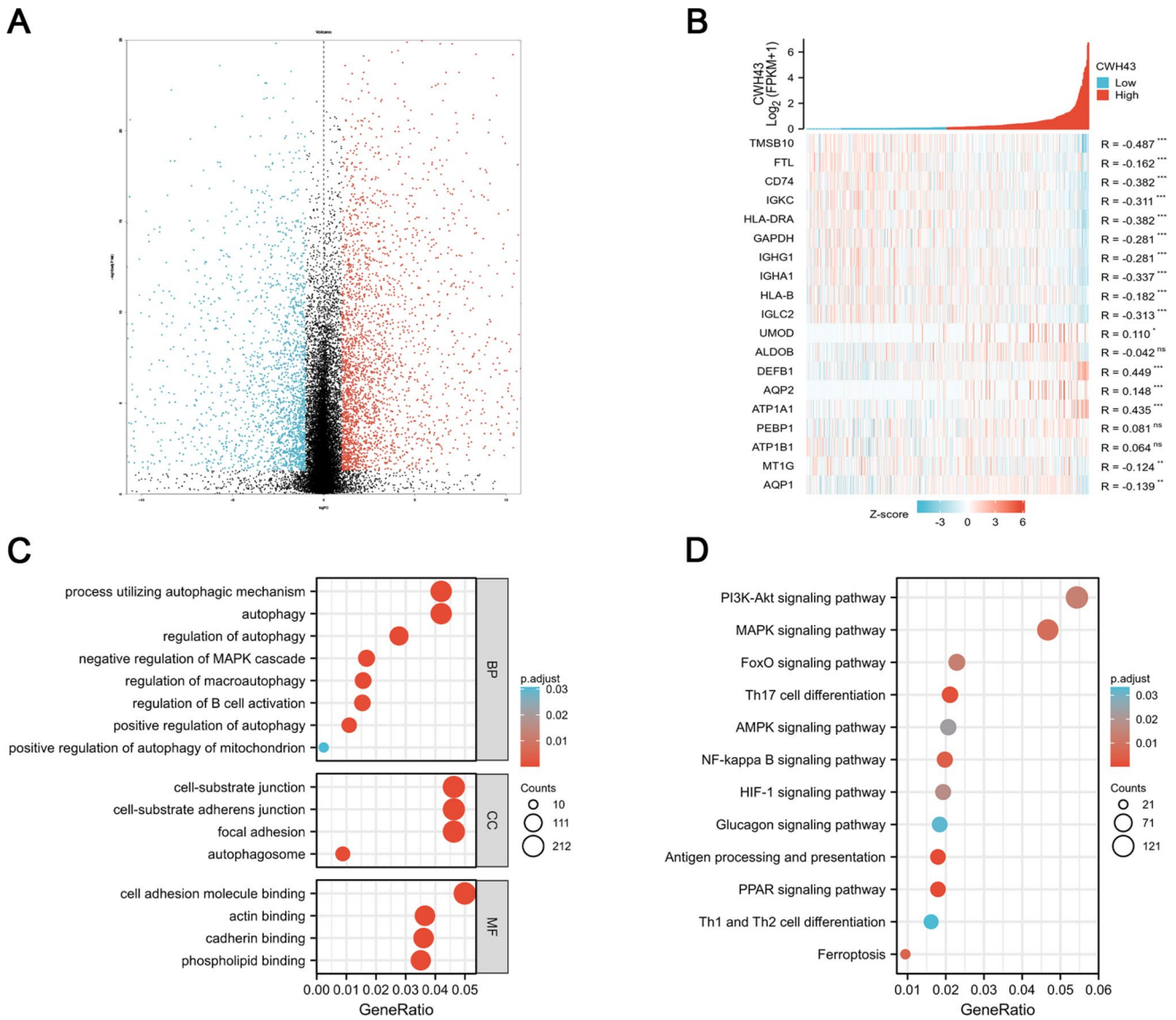

Fig. 11 Gene Expression Profiling Linked to CWH43 in ccRCC. **A** Heat map of 2776 up-regulated and 2211 down-regulated genes. **B** Focused heat map of 10 most significantly altered RNAs. **C** GO analysis of biological processes associated with CWH43. **D** KEGG pathway annotations

Additionally, to assess the impact of CWH43 expression levels on autophagic activity, we segregated 539 ccRCC samples into two groups: 270 with high CWH43 expression and 269 with low expression. We then compared the expression levels of key autophagy-related genes between these groups. The analysis demonstrated that genes such as MAP1LC3B, ATG14, ATG101, ATG3, ATG4 A, ATG2B, ATG5, and ATG4D were upregulated in the group with low CWH43 expression ($P < 0.05$) compared to the high expression group (Fig. 12J).

These findings underscore the integral relationship between CWH43 expression and the regulation of autophagy in ccRCC, suggesting that CWH43 may influence tumor behavior through modulation of autophagic pathways.

4 Discussion

CWH43, located on chromosome 4, plays a crucial role in the cellular distribution of glycosylated phosphatidylinositol-anchored proteins (GPI-AP) [37]. Identified in 2001 [38], CWH43 has predominantly been studied in yeast, where it impacts membrane targeting of GPI-AP [8, 39, 40]. There has been limited research on its implications in human health, such as its potential involvement in conditions like normal pressure hydrocephalus [37, 41]. However, with

Fig. 12 CWH43 and Autophagy in ccRCC. **A** Correlations between CWH43 expression and autophagy-related gene expression. **B**-**I** Scatter ▶ plots for the top 8 autophagy-related genes correlated with CWH43. **J** Comparative expression of autophagy-related genes between high and low CWH43 expression groups. Significance levels are marked accordingly

the advent of genome-wide microarray and high-throughput sequencing technologies, there has been a significant advancement in cancer research, particularly in areas like early diagnosis, cancer grading, and prognosis prediction [42]. These bioinformatics tools have enabled a deeper exploration of the complex molecular mechanisms and biological processes underlying cancer, prompting researchers to examine CWH43's specific roles in oncology. For instance, Zhang et al. observed significant downregulation of CWH43 in primary and metastatic gastric cancers [43], while Li et al. identified it as a central gene in gastric cancer through weighted gene co-expression network analysis, suggesting its utility as a biomarker for diagnosis and treatment [44]. Despite these findings, the research on CWH43 in cancer remains sparse, with few studies addressing its expression levels, potential prognostic value, and, crucially, its underlying molecular, epigenetic, and immunological mechanisms in tumor pathophysiology. Given this context, our study aims to fill the gap in understanding the prognostic value and potential roles of CWH43 in clear cell renal cell carcinoma (ccRCC), marking it as a focal point for uncovering novel therapeutic and diagnostic approaches in this malignancy. This investigation into CWH43's role in ccRCC could provide critical insights into its broader implications in cancer biology.

In this research, we initially focused on exploring the influence of CWH43 expression on the development and prognosis of clear cell renal cell carcinoma (ccRCC) by utilizing various comprehensive databases including TCGA, GEO, and the Human Protein Atlas. Our findings indicate a pronounced reduction in both mRNA and protein levels of CWH43 in ccRCC tissues compared to their normal counterparts. This observation suggests that ccRCC may suppress CWH43 expression, implying a potential tumor-suppressive role for CWH43 in this cancer type. Further analyses demonstrated significant correlations between CWH43 expression and various clinical parameters such as age, gender, T stage, M stage, pathological stage, and histological grade in ccRCC patients. These correlations could have substantial implications for tailoring immunotherapy approaches based on distinct clinicopathological profiles. Additionally, we assessed the prognostic significance of CWH43, finding it to be a strong predictor of overall survival (OS), disease-specific survival (DSS), progression-free interval (PFI), and disease-free survival (DFS) in ccRCC patients. Receiver operating characteristic (ROC) analysis further confirmed the diagnostic utility of CWH43. To enhance clinical applicability, we developed a prognostic nomogram that incorporates CWH43 along with other critical factors such as age, gender, race, T stage, M stage, N stage, pathological stage, histological grade, and laterality. This nomogram simplifies complex statistical models into a usable tool for predicting OS probabilities at 1-year, 3-year, and 5-year intervals. The calibration curves of our nomogram showed strong concordance between predicted and actual outcomes, enhancing its potential utility in clinical settings by providing individualized risk assessments for ccRCC patients. In conclusion, our study positions CWH43 as a promising diagnostic and prognostic biomarker for ccRCC, highlighting its potential to significantly influence patient management and treatment outcomes.

DNA methylation, particularly at the 5-carbon position of the cytosine ring within CpG dinucleotides in promoter and/or enhancer regions, plays a critical role in the regulation of gene expression and has been implicated in the development and progression of renal cell carcinoma (RCC). This epigenetic alteration, specifically hypermethylation of CpG sites, often leads to the inactivation of key tumor suppressor genes, thereby promoting tumor cell proliferation, invasion, and metastasis [46]. Our analysis using the Ualcan database revealed that patients with clear cell renal cell carcinoma (ccRCC) who exhibited hypermethylation of the CWH43 gene presented with more advanced disease stages and grades. Additionally, we observed that methylation levels of CWH43 were associated with patient demographics, including age, race, and gender. The findings from the Cancer Genome Atlas Research Network also support this observation, showing a general trend where increased promoter hypermethylation correlates with higher tumor stage and grade in ccRCC [47]. Further, our study examined the methylation status of 12 specific CpG sites within the CWH43 gene (cg03170472, cg11935592, cg24060908, cg22930650, cg13693941, cg18280362, cg08529049, cg04005707, cg24534566, cg25484904, cg22826333, and cg25316310). Notably, hypermethylation at most of these CpG loci was linked to poorer overall survival (OS) in patients, suggesting that DNA hypermethylation at these sites may contribute to the downregulation of CWH43 expression in ccRCC. Approximately 60% of ccRCC patients harbor mutated or inactivated von Hippel-Lindau (VHL) genes, a mutation widely recognized as a hallmark of ccRCC pathogenesis [48]. Interestingly, in our study, we found mutations in the CWH43 gene in a small subset of ccRCC patients, who also showed poorer OS compared to those without such mutations. However, given the limited sample size of patients with CWH43 mutations, further research is needed to ascertain whether mutations in the CWH43 gene could serve as a reliable biomarker for ccRCC. This exploration underscores the

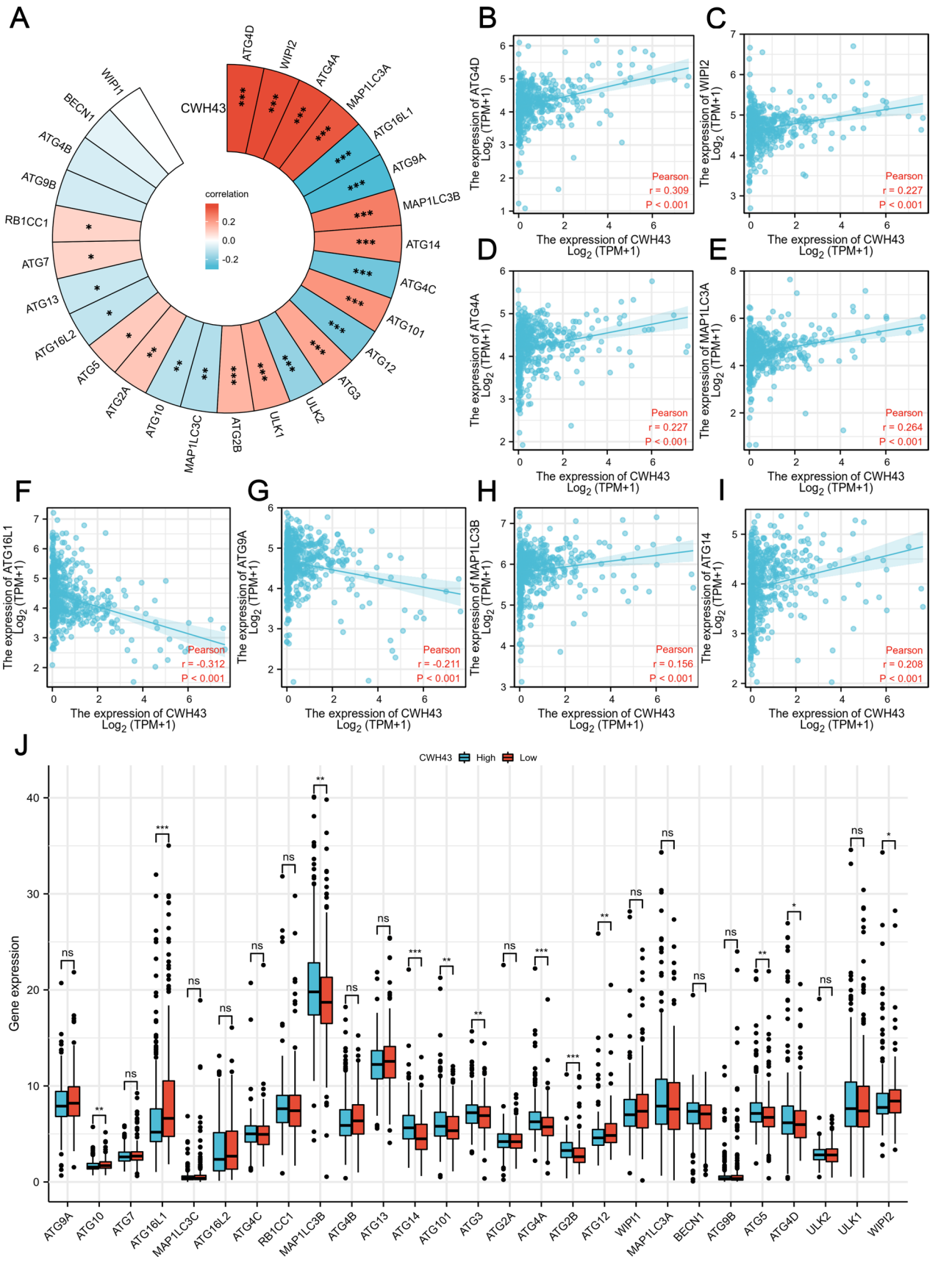
A
CWH43
correlation
0.2
0.0
-0.2
ATG4D
WIPI2
ATG4A
MAP1LC3A
ATG16L1
ATG9A
MAP1LC3B
ATG14
ATG4C
ATG101
ATG12
ATG3
ULK2
ULK1
ATG2B
MAP1LC3C
ATG10
ATG2A
ATG5
ATG16L2
ATG13
ATG7
RB1CC1
ATG9B
ATG4B
BECN1
WIPI1
B
The expression of ATG4D Log2 (TPM+1)
Pearson
r = 0.309
P < 0.001
The expression of CWH43 Log2 (TPM+1)
C
The expression of WIPI2 Log2 (TPM+1)
Pearson
r = 0.227
P < 0.001
D
The expression of ATG4A Log2 (TPM+1)
Pearson
r = 0.227
P < 0.001
E
The expression of MAP1LC3A Log2 (TPM+1)
Pearson
r = 0.264
P < 0.001
F
The expression of ATG16L1 Log2 (TPM+1)
Pearson
r = -0.312
P < 0.001
G
The expression of ATG9A Log2 (TPM+1)
Pearson
r = -0.211
P < 0.001
H
The expression of MAP1LC3B Log2 (TPM+1)
Pearson
r = 0.156
P < 0.001
I
The expression of ATG14 Log2 (TPM+1)
Pearson
r = 0.208
P < 0.001
J
CWH43 High Low
Gene expression
ATG9A ATG10 ATG7 ATG16L1 MAP1LC3C ATG16L2 ATG4C RB1CC1 MAP1LC3B ATG4B ATG13 ATG14 ATG101 ATG3 ATG2A ATG4A ATG2B ATG12 WIPI1 MAP1LC3A BECN1 ATG9B ATG5 ATG4D ULK2 ULK1 WIPI2

complexity of epigenetic and genetic interactions in ccRCC and highlights the potential of CWH43 as a significant factor in the disease's pathology. Further studies are required to fully understand the role of CWH43 in ccRCC and its utility in clinical practice.

Sunitinib is established as the primary therapeutic option for treating clear cell renal cell carcinoma (ccRCC) [49]. Research has demonstrated that combining sunitinib with saracatinib can synergistically curb the proliferation and migration of renal cell carcinoma cells [50]. Furthermore, Geng et al. have pinpointed dasatinib as a potent anti-ccRCC agent, confirming its antitumor efficacy through comprehensive in vitro and in vivo studies [51]. Our findings indicate a significant negative correlation between CWH43 expression and the responsiveness of ccRCC cells to several anticancer drugs, including saracatinib and dasatinib. This suggests that lower levels of CWH43 may impair the effectiveness of chemotherapy in ccRCC patients. Consequently, understanding the expression profile of CWH43 could be crucial for optimizing therapeutic strategies and potentially enhancing the response to treatment in ccRCC. This insight underlines the importance of further investigating the molecular interactions and pathways influenced by CWH43 to potentially adjust and improve therapeutic approaches for ccRCC..

The cancer immune cycle exemplifies the human immune system's response to malignancies, with its activity reflecting the cumulative impact of intricate immunomodulatory interactions within the tumor microenvironment (TME) [52]. Our research identified that most steps of the immune cycle were upregulated in the CWH43 low expression group, suggesting heightened immune activity. Additionally, there was notably higher infiltration of T follicular helper (Tfh) cells, regulatory T cells (Tregs), natural killer (NK) cells, and dendritic cells in this group. This enhanced infiltration aligns with the upregulation of suppressive immune checkpoint molecules such as CTLA-4, LAG3, and TIGIT, which are known to diminish immune cell activity and are key characteristics of an inflammatory TME [53]. Further analysis revealed elevated enrichment scores for pathways predictive of immunotherapy responses in the CWH43 low expression group, indicating a more pronounced immune infiltration status. This suggests that patients with low CWH43 expression are likely situated within an inflammatory TME. Recent predictions by Stein et al. suggest that the upcoming first-line therapies for kidney cancer may include combinations of PD-1/PD-L1 inhibitors with tyrosine kinase inhibitors (TKIs) or anti-CTLA-4 therapies [54]. Inhibition of CTLA-4, for instance, could weaken Treg function, enhancing the anti-tumor immune response. Moreover, a phase III study by Motzer et al. highlighted the effectiveness of dual targeting PD-1/PD-L1 and CTLA-4 in untreated patients with advanced renal cell carcinoma at intermediate or low risk [55]. Additionally, LAG3 not only hampers the activation of effector T cells but also enhances the suppressive capabilities of Tregs [56, 57]. With ongoing clinical trials and developments in therapies targeting other checkpoints like LAG-3, TIM-3, and TIGIT [58], our findings suggest that CWH43 expression levels could serve as valuable indicators for tailoring more effective antitumor immunotherapies for patients, potentially guiding therapeutic decisions towards interventions that leverage the inflammatory TME for improved clinical outcomes.

Currently, the role of CWH43 within tumor biology remains inadequately defined. To address this, we utilized Gene Ontology (GO) and Kyoto Encyclopedia of Genes and Genomes (KEGG) analyses to hypothesize how CWH43 might influence the progression of clear cell renal cell carcinoma (ccRCC). These analyses identified several autophagy-related processes potentially linked to CWH43, including autophagic mechanisms and the formation of autophagic vesicles. Intriguingly, KEGG analysis indicated connections between CWH43 and several critical signaling pathways: PI3 K-Akt, MAPK, FoxO, and AMPK, all of which are pivotal in cellular regulatory networks. The PI3 K/AKT pathway is well-documented for its role in modulating autophagy within tumors [33, 59], while the MAPK pathway is also recognized as a potential regulator of autophagy [60]. In our investigations, we examined the association between CWH43 expression and autophagy in ccRCC. We observed an upregulation in the expression of key autophagy-related genes including MAP1LC3B, ATG14, ATG101, ATG3, ATG4 A, ATG2B, ATG5, and ATG4D in the low CWH43 expression group, with CWH43 showing a significant positive correlation with most of these autophagy genes. Consequently, we propose that CWH43 may have a direct or indirect role in the autophagy pathways of ccRCC, potentially influencing the disease's progression. However, the link between CWH43 expression and autophagy has been derived primarily through bioinformatic analyses, necessitating further experimental validation to substantiate these findings.

To the best of our knowledge, this study represents the first in-depth analysis examining the links between CWH43 expression and various aspects such as prognosis, epigenetics, immunological function, and autophagy in patients with clear cell renal cell carcinoma (ccRCC). While this research enhances our comprehension of CWH43's role within ccRCC, it undoubtedly possesses several limitations. First, there is inherent variability in microarray and sequencing data across different databases, which might lack detailed granularity and specificity, potentially introducing systematic biases. Second, although we have experimentally confirmed the differential expression of CWH43 in ccRCC, further investigations are required to elucidate its mechanistic roles in the disease fully. Third, our current

data does not conclusively demonstrate that CWH43 directly modulates immune responses. Looking forward, more comprehensive prospective studies are essential to uncover the specific pathways through which CWH43 influences the biological behavior of ccRCC and its involvement in cancer immune infiltration. These studies will be crucial for developing innovative anti-tumor immunotherapeutic agents that target CWH43. In conclusion, we anticipate that the insights garnered from our findings will aid in the advancement of new immunotherapeutic targets, assist clinicians in selecting suitable therapeutic and prognostic biomarkers for ccRCC patients, and help in identifying biomarkers that can more precisely predict patient outcomes in ccRCC.

5 Conclusion

CWH43 is underexpressed in clear cell renal cell carcinoma (ccRCC) and its low expression correlates with poor patient outcomes. Hyper methylation of CWH43 is linked to both its downregulation and to a worse prognosis. Additionally, CWH43's negative correlation with the efficacy of various anticancer drugs suggests its involvement in chemoresistance. We also discovered that CWH43 contributes to an inflammatory tumor microenvironment (TME) in ccRCC. Given these findings, CWH43 shows promise as a prognostic biomarker for ccRCC and as a potential target for immunotherapy. Further research is needed to explore CWH43's mechanisms and therapeutic potential fully.

Author contributions AW and TZ conceived the study. AW, PB, HQ and TZ drafted the manuscript. AW performed the literature search and collected the data. AW and TZ analyzed and visualized the data. HQ and TZ revised the manuscript and were supporters of the study. All authors reviewed and approved the final manuscript.

Funding This study was supported by the Qinglan Project Excellent Teaching Team Fund of Yangzhou Polytechnic College and the Jiangsu Province Qinglan Project Academic Leaders Fund for Young and Middle-Aged Scholars.

Data availability The datasets analyzed for this study can be found in publicly accessible repositories. The genomic and clinical data were derived from The Cancer Genome Atlas (TCGA) available at TCGA portal and gene expression data from the Gene Expression Omnibus (GEO) accessible at GEO database. These datasets were used under open access terms without restrictions on their use for research purposes.

Declarations

Competing interests The authors declare no competing interests.

10 References

1. Bray F, Ferlay J, Soerjomataram I, Siegel RL, Torre LA, Jemal A. Global cancer statistics 2018: GLOBOCAN estimates of incidence and mortality worldwide for 36 cancers in 185 countries. CA Cancer J Clin. 2018;68:394–424.
2. Capitanio U, Montorsi F. Renal cancer. Lancet (London England). 2016;387:894–906.
3. Bhatt JR, Finelli A. Landmarks in the diagnosis and treatment of renal cell carcinoma. Nat Rev Urol. 2014;11:517–25.
4. Siegel RL, Miller KD, Jemal A. Cancer statistics, 2019. CA Cancer J Clin. 2019;69:7–34.
5. Awakura Y, Nakamura E, Ito N, Kamoto T, Ogawa O. Methylation-associated silencing of SFRP1 in renal cell carcinoma. Oncol Rep. 2008;20:1257–63.
6. Topalian SL, Hodi FS, Brahmer JR, Gettinger SN, Smith DC, McDermott DF, Powderly JD, Sosman JA, Atkins MB, Leming PD, Spigel DR, Antonia SJ, Drilon A, Wolchok JD, Carvajal RD, McHenry MB, Hosein F, Harbison CT, Grosso JF, Sznol M. Five-year survival and correlates among patients with advanced melanoma, renal cell carcinoma, or non-small cell lung cancer treated with nivolumab. JAMA Oncol. 2019;5:1411–20.

7. Xiong J, et al. The two-sided battlefield of tumour-associated macrophages in glioblastoma: unravelling their therapeutic potential. Discov Oncol. 2024;15(1):590. https://doi.org/10.1007/s12672-024-01464-5.
8. Ghugtyal V, Vionnet C, Roubaty C, Conzelmann A. CWH43 is required for the introduction of ceramides into GPI anchors in Saccharomyces cerevisiae. Mol Microbiol. 2007;65:1493–502.
9. Laczmanska I, Sasiadek M, Laczmanski L. The comparison between molecular tumour profiling in microdissected and surgical tissue samples. Anticancer Res. 2018;38:1415–8.
10. Chu CM, Yao CT, Chang YT, Chou HL, Chou YC, Chen KH, Terng HJ, Huang CS, Lee CC, Su SL, Liu YC, Lin FG, Wetter T, Chang CW. Gene expression profiling of colorectal tumors and normal mucosa by microarrays meta-analysis using prediction analysis of microarray, artificial neural network, classification, and regression trees. Dis Mark. 2014;2014: 634123.
11. Sapkota S, Horiguchi K, Tosaka M, Yamada S, Yamada M. Whole-exome sequencing study of thyrotropin-secreting pituitary adenomas. J Clin Endocrinol Metab. 2017;102:566–75.
12. Ye B, Fan D, Xiong W, Li M, Yuan J, Jiang Q, Zhao Y, Lin J, Liu J, Lv Y, Wang X, Li Z, Su J, Qiao Y. Oncogenic enhancers drive esophageal squamous cell carcinogenesis and metastasis. Nat Commun. 2021;12:4457.
13. Vivian J, Rao AA, Nothaft FA, Ketchum C, Armstrong J, Novak A, Pfeil J, Narkizian J, Deran AD, Musselman-Brown A, Schmidt H, Amstutz P, Craft B, Goldman M, Rosenbloom K, Cline M, O'Connor B, Hanna M, Birger C, Kent WJ, Patterson DA, Joseph AD, Zhu J, Zaranek S, Getz G, Haussler D, Paten B. Toil enables reproducible, open source, big biomedical data analyses. Nat Biotechnol. 2017;35:314–6.
14. Davis S, Meltzer PS. GEOquery: a bridge between the Gene expression omnibus (GEO) and BIOCOnductor. Bioinformatics (Oxford England). 2007;23:1846–7.
15. Wang NN, Dong J, Zhang L, Ouyang D, Cheng Y, Chen AF, Lu AP, Cao DS. HAMdb: a database of human autophagy modulators with specific pathway and disease information. J Cheminformatics. 2018;10:34.
16. Liu J, Lichtenberg T, Hoadley KA, Poisson LM, Lazar AJ, Cherniack AD, Kovatich AJ, Benz CC, Levine DA, Lee AV, Omberg L, Wolf DM, Shriver CD, Thorsson V, Hu H. An integrated TCGA pan-cancer clinical data resource to drive high-quality survival outcome analytics. Cell. 2018;173:400-416.e11.
17. Tang Z, Li C, Kang B, Gao G, Li C, Zhang Z. GEPIA: a web server for cancer and normal gene expression profiling and interactive analyses. Nucl Acid Res. 2017;45:W98-w102.
18. Chandrashekar DS, Bashel B, Balasubramanya SAH, Creighton CJ, Ponce-Rodriguez I, Chakravarthi B, Varambally S. UALCAN: a portal for facilitating tumor subgroup gene expression and survival analyses. Neoplasia (New York NY). 2017;19:649–58.
19. Modhukur V, Iljasenko T, Metsalu T, Lokk K, Laisk-Podar T, Vilo J. MethSurv: a web tool to perform multivariable survival analysis using DNA methylation data. Epigenomics. 2018;10:277–88.
20. Gao J, Aksoy BA, Dogrusoz U, Dresdner G, Gross B, Sumer SO, Sun Y, Jacobsen A, Sinha R, Larsson E, Cerami E, Sander C, Schultz N. Integrative analysis of complex cancer genomics and clinical profiles using the cBioPortal. Sci Signal. 2013. https://doi.org/10.1126/scisignal.2004088.
21. Shankavaram UT, Varma S, Kane D, Sunshine M, Chary KK, Reinhold WC, Pommier Y, Weinstein JN. Cell miner: a relational database and query tool for the NCI-60 cancer cell lines. BMC Genom. 2009;10:277.
22. Reinhold WC, Sunshine M, Liu H, Varma S, Kohn KW, Morris J, Doroshow J, Pommier Y. Cell miner: a web-based suite of genomic and pharmacologic tools to explore transcript and drug patterns in the NCI-60 cell line set. Can Res. 2012;72:3499–511.
23. Charoentong P, Finotello F, Angelova M, Mayer C, Efremova M, Rieder D, Hackl H, Trajanoski Z. Pan-cancer immunogenomic analyses reveal genotype-immunophenotype relationships and predictors of response to checkpoint blockade. Cell Rep. 2017;18:248–62.
24. Xu L, Deng C, Pang B, Zhang X, Liu W, Liao G, Yuan H, Cheng P, Li F, Long Z, Yan M, Zhao T, Xiao Y, Li X. TIP: a web server for resolving tumor immunophenotype profiling. Can Res. 2018;78:6575–80.
25. Mariathasan S, Turley SJ, Nickles D, Castiglioni A, Yuen K, Wang Y, Kadel EE III, Koeppen H, Astarita JL, Cubas R, Jhunjhunwala S, Banchereau R, Yang Y, Guan Y, Chalouni C, Ziai J, Şenbabaoğlu Y, Santoro S, Sheinson D, Hung J, Giltnane JM, Pierce AA, Mesh K, Lianoglou S, Riegler J, Carano RAD, Eriksson P, Höglund M, Somarriba L, Halligan DL, van der Heijden MS, Loriot Y, Rosenberg JE, Fong L, Mellman I, Chen DS, Green M, Derleth C, Fine GD, Hegde PS, Bourgon R, Powles T. TGFβ attenuates tumour response to PD-L1 blockade by contributing to exclusion of T cells. Nature. 2018;554:544–8.
26. Chen B, Khodadoust MS, Liu CL, Newman AM, Alizadeh AA. Profiling tumor infiltrating immune cells with CIBERSORT. Method Mol Biol (Clifton NJ). 2018;1711:243–59.
27. Smyth GK. Linear models and empirical bayes methods for assessing differential expression in microarray experiments. Statistical Appl Gen Mol Biol. 2004;3: Article3.
28. Yu G, Wang LG, Han Y, He QY. clusterProfiler: an R package for comparing biological themes among gene clusters. OMICS. 2012;16:284–7.
29. Feinberg AP, Tycko B. The history of cancer epigenetics. Nat Rev Cancer. 2004;4:143–53.
30. Chen DS, Mellman I. Oncology meets immunology: the cancer-immunity cycle. Immunity. 2013;39:1–10.
31. Kerkar SP, Restifo NP. Cellular constituents of immune escape within the tumor microenvironment. Can Res. 2012;72:3125–30.
32. Pardoll DM. The blockade of immune checkpoints in cancer immunotherapy. Nat Rev Cancer. 2012;12:252–64.
33. Ma Z, Lou S, Jiang Z. PHLDA2 regulates EMT and autophagy in colorectal cancer via the PI3K/AKT signaling pathway. Aging. 2020;12:7985–8000.
34. Fan J, Ren D, Wang J, Liu X, Zhang H, Wu M, Yang G. Bruceine D induces lung cancer cell apoptosis and autophagy via the ROS/MAPK signaling pathway in vitro and in vivo. Cell Death Dis. 2020;11:126.
35. Farhan M, Silva M, Li S, Yan F, Fang J, Peng T, Hu J, Tsao MS, Little P, Zheng W. The role of FOXOs and autophagy in cancer and metastasis-Implications in therapeutic development. Med Res Rev. 2020;40:2089–113.
36. Chen M, Zhang S, Nie Z, Wen X, Gao Y. Identification of an autophagy-related prognostic signature for clear cell renal cell carcinoma. Front Oncol. 2020;10:873.
37. Yang HW, Lee S, Yang D, Dai H, Zhang Y, Han L, Zhao S, Zhang S, Ma Y, Johnson MF, Rattray AK, Johnson TA, Wang G, Zheng S, Carroll RS, Park PJ, Johnson MD. Deletions in CWH43 cause idiopathic normal pressure hydrocephalus. EMBO Mol Med. 2021;13: e13249.

38. Nokelainen M, Tu H, Vuorela A, Notbohm H, Kivirikko KI, Myllyharju J. High-level production of human type I collagen in the yeast Pichia pastoris. Yeast (Chichester England). 2001;18:797–806.
39. Nakazawa N, Teruya T, Sajiki K, Kumada K, Villar-Briones A, Arakawa O, Takada J, Saitoh S, Yanagida M. The putative ceramide-conjugation protein Cwh43 regulates G0 quiescence, nutrient metabolism and lipid homeostasis in fission yeast. J Cell Sci. 2018. https://doi.org/10.1242/jcs.217331.
40. Nakazawa N, Xu X, Arakawa O, Yanagida M. Coordinated roles of the putative ceramide-conjugation protein, Cwh43, and a Mn(2+)-transporting, P-Type ATPase, Pmr1, in fission yeast. G3 (Bethesda Md). 2019;9:2667–76.
41. Yang D, Yang H, Luiselli G, Ogagan C, Dai H, Chiu L, Carroll RS, Johnson MD. Increased plasmin-mediated proteolysis of L1CAM in a mouse model of idiopathic normal pressure hydrocephalus. Proceed Natl Acad Sci U S A. 2021. https://doi.org/10.1073/pnas.2010528118.
42. Kulasingam V, Diamandis EP. Strategies for discovering novel cancer biomarkers through utilization of emerging technologies. Nat Clin Pract Oncol. 2008;5:588–99.
43. Zhang J, Huang JY, Chen YN, Yuan F, Zhang H, Yan FH, Wang MJ, Wang G, Su M, Lu G, Huang Y, Dai H, Ji J, Zhang J, Zhang JN, Jiang YN, Chen SJ, Zhu ZG, Yu YY. Whole genome and transcriptome sequencing of matched primary and peritoneal metastatic gastric carcinoma. Sci Rep. 2015;5:13750.
44. Li C, Yu H, Sun Y, Zeng X, Zhang W. Identification of the hub genes in gastric cancer through weighted gene co-expression network analysis. PeerJ. 2021;9: e10682.
45. Park SY. Nomogram: an analogue tool to deliver digital knowledge. J Thorac Cardiovasc Surg. 2018;155:1793.
46. Shenoy N, Vallumsetla N, Zou Y, Galeas JN, Shrivastava M, Hu C, Susztak K, Verma A. Role of DNA methylation in renal cell carcinoma. J Hematol Oncol. 2015;8:88.
47. Cancer Genome Atlas Research Network. Comprehensive molecular characterization of clear cell renal cell carcinoma. Nature. 2013;499(7456):43–9. https://doi.org/10.1038/nature12222.
48. An J, Rettig MB. Mechanism of von Hippel-Lindau protein-mediated suppression of nuclear factor kappa B activity. Mol Cell Biol. 2005;25:7546–56.
49. Park SE, Kim W, Hong JY, Kang D, Park S, Suh J, You D, Park YY, Suh N, Hwang JJ, Kim CS. miR-96-5p targets PTEN to mediate sunitinib resistance in clear cell renal cell carcinoma. Sci Rep. 2022;12:3537.
50. Zhang S, Yu D. Targeting Src family kinases in anti-cancer therapies: turning promise into triumph. Trend Pharmacol Sci. 2012;33:122–8.
51. Sun J, Wang X, Tang B, Liu H, Zhang M, Wang Y, Ping F, Ding J, Shen A, Geng M. A tightly controlled Src-YAP signaling axis determines therapeutic response to dasatinib in renal cell carcinoma. Theranostics. 2018;8:3256–67.
52. Hu J, Yu A, Othmane B, Qiu D, Li H, Li C, Liu P, Ren W, Chen M, Gong G, Guo X, Zhang H, Chen J, Zu X. Siglec15 shapes a non-inflamed tumor microenvironment and predicts the molecular subtype in bladder cancer. Theranostics. 2021;11:3089–108.
53. Spranger S, Spaapen RM, Zha Y, Williams J, Meng Y, Ha TT, Gajewski TF. Up-regulation of PD-L1, IDO, and T(regs) in the melanoma tumor microenvironment is driven by CD8(+) T cells. Sci Trans Med. 2013;5:200ra116.
54. Drake CG, Stein MN. The immunobiology of kidney cancer. J Clin Oncol. 2018. https://doi.org/10.1200/JCO.2018.79.2648.
55. Motzer RJ, Rini BI, McDermott DF, Arén Frontera O, Hammers HJ, Carducci MA, Salman P, Escudier B, Beuselinck B, Amin A, Porta C, George S, Neiman V, Bracarda S, Tykodi SS, Barthélémy P, Leibowitz-Amit R, Plimack ER, Oosting SF, Redman B, Melichar B, Powles T, Nathan P, Oudard S, Pook D, Choueiri TK, Donskov F, Grimm MO, Gurney H, Heng DYC, Kollmannsberger CK, Harrison MR, Tomita Y, Duran I, Grünwald V, McHenry MB, Mekan S, Tannir NM. Nivolumab plus ipilimumab versus sunitinib in first-line treatment for advanced renal cell carcinoma: extended follow-up of efficacy and safety results from a randomised, controlled, phase 3 trial. Lancet Oncol. 2019;20:1370–85.
56. Andrews LP, Marciscano AE, Drake CG, Vignali DA. LAG3 (CD223) as a cancer immunotherapy target. Immunol Rev. 2017;276:80–96.
57. Turnis ME, Andrews LP, Vignali DA. Inhibitory receptors as targets for cancer immunotherapy. Eur J Immunol. 2015;45:1892–905.
58. Takamatsu K, Tanaka N, Hakozaki K, Takahashi R, Teranishi Y, Murakami T, Kufukihara R, Niwa N, Mikami S, Shinojima T, Sasaki T, Sato Y, Kume H, Ogawa S, Kakimi K, Kamatani T, Miya F, Tsunoda T, Aimono E, Nishihara H, Sawada K, Imamura T, Mizuno R, Oya M. Profiling the inhibitory receptors LAG-3, TIM-3, and TIGIT in renal cell carcinoma reveals malignancy. Nat Commun. 2021;12:5547.
59. Yang J, Pi C, Wang G. Inhibition of PI3K/Akt/mTOR pathway by apigenin induces apoptosis and autophagy in hepatocellular carcinoma cells. Biomed Pharmacother Biomed Pharmacother. 2018;103:699–707.
60. Zhou YY, Li Y, Jiang WQ, Zhou LF. MAPK/JNK signalling: a potential autophagy regulation pathway. 2015. Biosci Rep. https://doi.org/10.1042/BSR20140141.